



HAL
open science

Exploration of a European-centered strawberry diversity panel provides markers and candidate genes for the control of fruit quality traits

Alexandre Prohaska, Pol Rey-Serra, Johann J. Petit, Aurélie Petit, Justine Perrotte, Christophe Rothan, Béatrice Denoyes

► To cite this version:

Alexandre Prohaska, Pol Rey-Serra, Johann J. Petit, Aurélie Petit, Justine Perrotte, et al.. Exploration of a European-centered strawberry diversity panel provides markers and candidate genes for the control of fruit quality traits. *Horticulture research*, 2024, 10.1093/hr/uhae137/7672963 . hal-04612454

HAL Id: hal-04612454

<https://hal.inrae.fr/hal-04612454>

Submitted on 14 Jun 2024

HAL is a multi-disciplinary open access archive for the deposit and dissemination of scientific research documents, whether they are published or not. The documents may come from teaching and research institutions in France or abroad, or from public or private research centers.

L'archive ouverte pluridisciplinaire **HAL**, est destinée au dépôt et à la diffusion de documents scientifiques de niveau recherche, publiés ou non, émanant des établissements d'enseignement et de recherche français ou étrangers, des laboratoires publics ou privés.



Distributed under a Creative Commons Attribution 4.0 International License

1 Article Title

2 **Exploration of a European-centered strawberry diversity panel provides markers and candidate genes for**
3 **the control of fruit quality traits**

4
5 **Running title:** GWAS of strawberry quality traits and candidate genes

6
7 Alexandre Prohaska^{1,2}, Pol Rey-Serra¹, Johann Petit¹, Aurélie Petit², Justine Perrotte², Christophe Rothan^{1*},
8 Béatrice Denoyes^{1*}

9 ¹ Univ. Bordeaux, INRAE, UMR BFP, F-33140, Villenave d'Ornon, France.

10 ² Invenio, MIN de Brienne, 110 quai de Paludate, 33000 Bordeaux, France

11
12 * Corresponding authors:

13 **Béatrice Denoyes** <https://orcid.org/0000-0002-0369-9609>

14 Email: beatrice.denoyes@inrae.fr; Phone: +335 57 12 24 60

15 UMR BFP – INRAE, 71 avenue Edouard Bourlaux, 33140 Villenave d'Ornon, France

16 **Christophe Rothan** <https://orcid.org/0000-0002-6831-2823>

17 Email: christophe.rothan@inrae.fr; Phone: +335 57 12 24 60 ;

18 UMR BFP – INRAE, 71 avenue Edouard Bourlaux, 33140 Villenave d'Ornon, France

19
20 Alexandre Prohaska: alexandre.prohaska@gmail.com; <https://orcid.org/0009-0004-0395-7470>

21 Pol Rey-Serra: pol.rey-serra@inrae.fr; <https://orcid.org/0000-0002-3685-2470>

22 Johann Petit: johann.petit@inrae.fr; <https://orcid.org/0000-0002-6746-1755>

23 Aurélie Petit: a.petit@invenio-fl.fr; <https://orcid.org/0000-0003-1577-9072>

24 Justine Perrotte: j.perrotte@invenio-fl.fr

25 Christophe Rothan: christophe.rothan@inrae.fr; <https://orcid.org/0000-0002-6831-2823>

26 Béatrice Denoyes: beatrice.denoyes@inrae.fr; <https://orcid.org/0000-0002-0369-9609>

27
28
29 © The Author(s) 2024. Published by Oxford University Press. This is an Open Access article distributed

30 under the terms of the Creative Commons Attribution License

31 <https://creativecommons.org/licenses/by/4.0/>, which permits unrestricted reuse, distribution, and

32 reproduction in any medium, provided the original work is properly cited.

33

34 Abstract

35 Fruit quality traits are major breeding targets in cultivated strawberry (*Fragaria × ananassa*). Taking into
36 account the requirements of both growers and consumers when selecting high quality cultivars is a real
37 challenge. Here, we used a diversity panel enriched with unique European accessions and the 50K FanaSNP
38 array to highlight the evolution of strawberry diversity over the past 160 years, investigate the molecular
39 basis of 12 major fruit quality traits by Genome-Wide Association Studies (GWAS), and provide genetic
40 markers for breeding. Results show that considerable improvements of key breeding targets including fruit
41 weight, firmness, composition and appearance occurred simultaneously in European and American
42 cultivars. Despite the high genetic diversity of our panel, we observed a drop in nucleotide diversity in
43 certain chromosomal regions, revealing the impact of selection. GWAS identified 71 associations with 11
44 quality traits and, while validating known associations (firmness, sugar), highlighted the predominance of
45 new QTL, demonstrating the value of using untapped genetic resources. Three of the six selective sweeps
46 detected are related to glossiness or skin resistance, two little-studied traits important for fruit
47 attractiveness and, potentially, postharvest shelf-life. Moreover, major QTL for firmness, glossiness, skin
48 resistance and susceptibility to bruising are found within a low diversity region of chromosome 3D.
49 Stringent search for candidate genes underlying QTL uncovered strong candidates for fruit color, firmness,
50 sugar and acid composition, glossiness and skin resistance. Overall, our study provides a potential avenue
51 for extending shelf-life without compromising flavor and color as well as the genetic markers needed to
52 achieve this goal.

53

54 **Keywords:** *Fragaria × ananassa*, strawberry, diversity, fruit quality, GWAS, candidate genes

55

56

57 Introduction

58

59 Cultivated strawberry (*Fragaria × ananassa*), the most widely consumed small fruit worldwide, results from
60 spontaneous hybridization in botanical gardens in France in the 18th century between two octoploid ($2n =$
61 $8x = 56$) species (*F. chiloensis* and *F. virginiana*) imported from the New World¹. Since then, cultivated
62 strawberry has been continuously improved through the introgression of alleles from wild progenitors
63 creating an admixed population of interspecific hybrid lineages^{2,3,4}. Recurrent hybridization contributed to
64 maintain genetic diversity in the domesticated populations⁴. However, lower genetic diversity and
65 heterozygosity can be observed in highly structured populations, which nevertheless show considerably
66 improved yield, fruit weight and firmness⁵. Current efforts, triggered by consumer demand for sweet and
67 highly-flavored strawberries^{6,7}, are aimed at improving the sensory and nutritional quality traits of the fruit
68 such as color⁸ and flavor⁹. Another area for improvement is the extension of the storage period and the
69 reduction of post-harvest rot, both of which are linked to fruit firmness⁷ and little-explored fruit surface
70 properties¹⁰. Several fruit quality traits can be easily manipulated using advanced technology, such as
71 genome editing which has successfully been applied to create new alleles modifying various traits including
72 fruit color, sweetness and aroma^{7,11}. Other complex (e.g. fruit size) and/or little-studied (e.g. fruit
73 glossiness) traits first require elucidation of their genetic architecture. Until recently, following initial
74 studies^{12,13}, the dissection of the genetic control of complex fruit quality traits in *F. × ananassa* has mainly
75 been achieved by mapping Quantitative Trait Locus (QTL) on genetic linkage maps of bi-parental^{14,15,16} or
76 multi-parental¹⁷ populations. Causal genetic variants have been identified for several QTL, leading to the
77 design of genetic markers for marker-assisted selection (MAS) of strawberry varieties with, for example,
78 improved fruit color^{8,18} and better aroma⁹.

79

80 Complexity of the allo-octoploid genome of *F. × ananassa*, where up to eight homeo-allelic forms of the
81 same gene can be found¹⁹, has until recently hampered the mapping of QTLs on a given chromosome.
82 Whole genome sequencing of *F. × ananassa*¹ and, more recently, its progenitors²⁰, showed that the four
83 subgenomes of *F. × ananassa* are derived from the diploids *F. vesca* and *F. iinumae* and from two extinct
84 species related to *F. iinumae*^{20,21}. Genome sequence further enabled the design of a single nucleotide
85 polymorphism (SNP) 50K array with selected chromosome-specific SNPs²² allowing the high-resolution
86 mapping of QTLs. A recent breakthrough has been the completion of haplotype-resolved genomes for five
87 genotypes of *F. × ananassa*^{9,23,24,25,26}. These developments make it possible to exploit strawberry diversity
88 through genome wide association studies (GWAS), which scans the genome for significant associations
89 between genetic markers and the trait studied². It thus can help unveil beneficial alleles through the
90 exploration and characterization of strawberry genetic resources, which display a wide genetic and
91 phenotypic diversity^{4,27,28,29}. So far, GWAS has been done on collections mostly centered on North American

92 strawberry populations^{4,29}, which enabled the discovery of major QTLs controlling fruit weight, firmness,
93 sweetness and aroma^{4,9,29,30,31}. It would certainly benefit from the exploration of other less well-
94 characterized germplasm found in Europe³², a historically active strawberry breeding center⁶.

95

96 In this study, we explored by GWAS the genetic architecture of fruit quality in *F. × ananassa*. To this end, we
97 used the unexploited genetic diversity found in traditional and modern European varieties, in comparison
98 with the better described diversity of North American varieties and some Asian genotypes. Our results are
99 consistent with recent insights into the evolution of modern strawberry varieties and detected major QTL
100 recently described, for fruit firmness for example. Moreover, we detected new QTL for most of the 12 fruit
101 quality traits studied and the underlying candidate genes (CG). An example of this are the QTL and strong
102 CG for the little-explored glossy trait, which underpins the shiny appearance of all modern strawberry
103 varieties and was found to co-localize with a skin resistance trait. Our results therefore highlight the
104 richness of European collections as a source of genetic diversity for strawberry breeding.

105

106 Results

107

108 Population structure and genetic diversity of the diversity panel of cultivated strawberry

109 We analyzed a germplasm diversity panel comprising 223 accessions of cultivated strawberries (*F. ×*
110 *ananassa*) available at Invenio (South-West France) (Table S1). Unlike the main diversity panels studied to
111 date, where the bulk of the panel was constituted by North American accessions^{4,28}, our panel was mostly
112 composed of European accessions from several countries, with French cultivars being by far the most
113 represented (96 accessions). In addition, the panel comprised representative cultivars from North America
114 including California and Florida, Japan and other breeding programs around the world (Fig. 1A, Table S1).
115 Many cultivars were released between 1990s and nowadays, but the panel also accurately covered the
116 whole modern breeding period (>1950s) and the early stages of strawberry breeding, with cultivars
117 reaching as far as the beginning of the 19th century (Fig. S1). Thirty-two accessions from this panel were
118 common with those from the study by Horvath et al. (2011)³². Accessions from the diversity panel were
119 genotyped with the 50K FanaSNP array²². A total of 38,120 SNPs was retained after filtering for minor allelic
120 frequency (MAF) (< 5%) and missing data (> 3%).

121 To explore relationships among the 223 accessions, we first evaluated the population structure with
122 STRUCTURE software. We identified three distinct genetic clusters (Fig. 1B, Table S1). Group 1 (G1) includes
123 most of the older European cultivars and their more recent relatives, as well as some old American cultivars
124 (Fig. 1B). This group is hereafter named the Heirloom & related group. Group 2 (G2) clusters essentially
125 European, as well as 14 American cultivars mostly from North-East America (Maryland, New-York and
126 Canada) and three out of five Japanese cultivars (Fig. 1B) and was therefore named the European mixed

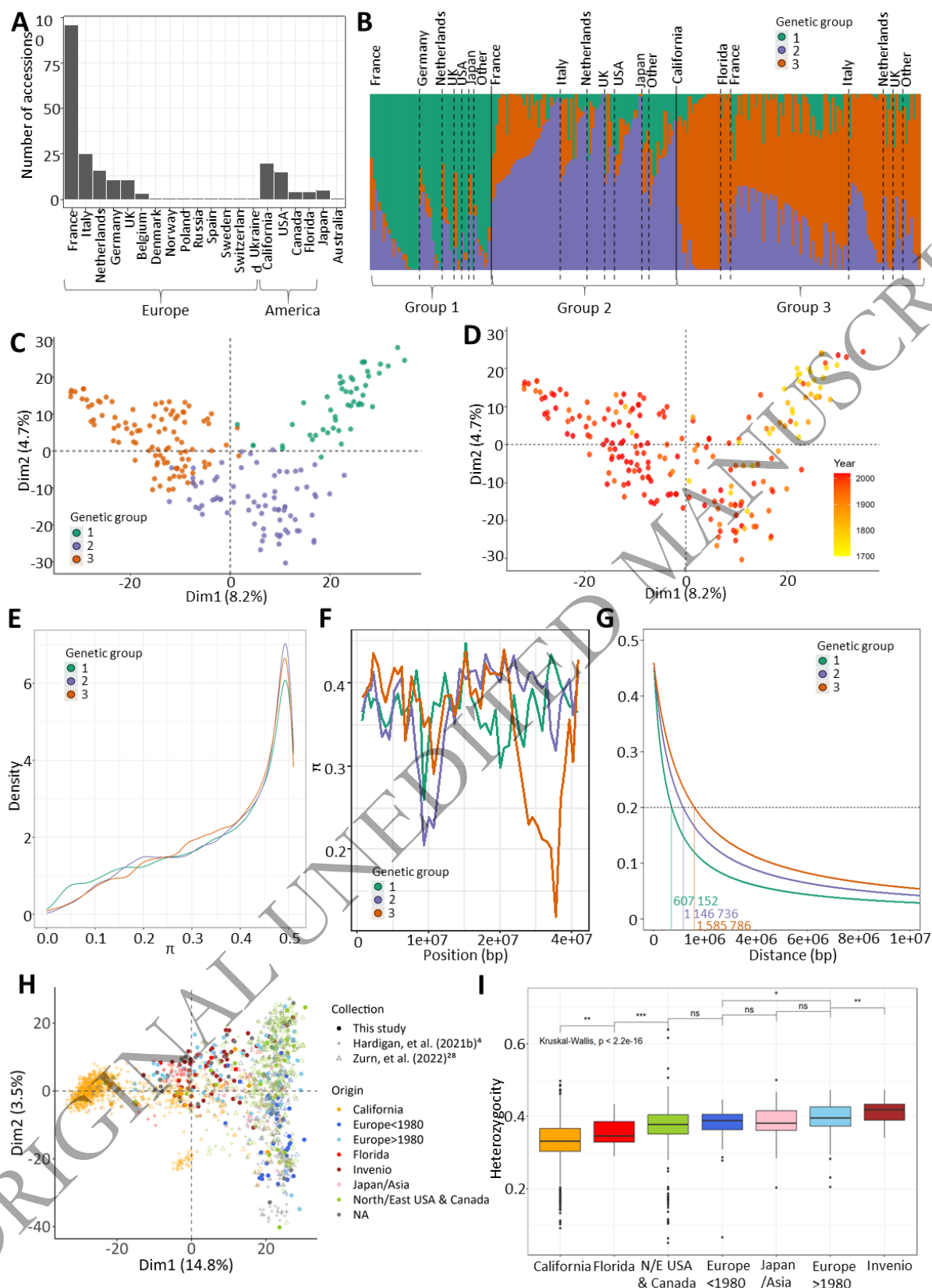
127 group. California and Florida cultivars, together with other European ones, have been identified in group 3
128 (G3) hereafter named the American & European mixed group. A large amount of admixture (< 70%) was
129 observed for each group, with 108 out of 223 accessions split across more than one group, with most of the
130 admixture spread between G2 and G3 (Fig. 1B).

131 To further investigate population structure, we performed principal component analysis (PCA) of the 223
132 accessions using the 38,120 SNP markers (Fig. 1C). The first two dimensions (PC1, PC2) explained 8.2% and
133 4.7% of the structural variance, respectively. The three genetic groups were positioned at each vertex of
134 the crescent shape. PC1 also reflected the temporal separation between G1 and the other two groups
135 when cultivars were displayed according to year of release (Fig. 1D). The phylogenetic analysis (Fig. S2) was
136 consistent with the structure (Fig. 1B) and PCA (Figs 1C, 1D) analyses.

137 Genome-wide comparisons of nucleotide diversity (π) between genetic groups revealed no clear loss of
138 genetic diversity from G1 to G2 and G3 (Fig. 1E). At the chromosome level, the distribution of nucleotide
139 diversity among groups was uneven, with several genomic regions associated with significant enrichment
140 or loss. Of notice, some regions were associated with a sharp reduction in diversity in G2 and/or G3
141 compared with G1, for example the 23,233 kb to 29,635 kb region on chromosome 3D (Fig. 1F). Additional
142 examples can be found on other chromosomes such as chromosomes 2C, 3B and 6B (Fig. S3). Progression
143 towards the most recent American and European cultivars also translated in local augmentation in linkage
144 disequilibrium, where LD (at $r^2 = 0.20$) increased from an average distance of 802,184 bp for G1 to
145 1,073,213 bp for G2 and 1,253,777 bp for G3 (Fig. 1G, Fig. S4).

146 We then combined the SNP data from our diversity panel with those from University of California Davis
147 (UCD panel)⁴ and United States Department of Agriculture (USDA panel)²⁷ to position our collection in
148 relation with these studies. The PCA of the combined data revealed that the Invenio collection largely
149 overlapped the two USA collections, with the exception of the extreme end of the PC1 corresponding to the
150 UCD program and a small group of genotypes representing probable introgressions of wild accessions into
151 the California panel (Fig. 1H, Fig. S5). The University of Florida (FL) program was less represented in the
152 dataset, and closer to the UCD program on the PCA. Japanese and Asian varieties were located at the
153 center of the crescent. In addition, the PCA highlighted the enrichment of our panel in unique
154 accessions not found in the UCD and USDA panel, thus emphasizing its potential to find new phenotypic
155 diversity for fruit quality traits in cultivated strawberry (Fig. 1H, Fig. S6). Heterozygosity decreased in
156 California and Florida cultivars in comparison to European and Asian cultivars. Interestingly, heterozygosity
157 was significantly higher in cultivars and advanced lines of Invenio and in recent European cultivars (released
158 after 1980) (Fig. 1I).

159



160

161

162

163

Figure 1. Genetic diversity of the panel. (A) Distribution of the geographical origin of the 223 accessions.

(B) Structure barplot representing each genotype (bars) by its percentage of affiliation to each of the three

genetic groups according to the STRUCTURE analysis. Individuals are sorted by genetic groups and

164 geographical origins. (C,D) Principal Component Analysis of 38,120 SNP markers. Each accession (dot) is
 165 colored by its genetic group (C) or year of release (D). (E) Nucleotide diversity (π) distributions in windows
 166 of 400 kb across each genetic group. (F) π chromosome-wide estimates for each genetic group for 400kb
 167 windows across the chromosome 3D. (G) Linkage disequilibrium (LD) decay along chromosome 1A. The
 168 dashed line represents the LD decay at $r^2=0.2$. (H) Distribution of the Invenio panel (filled dots) among
 169 1,569 genotypes (shaded dots) studied in Hardigan et al. (2021b)⁴ and 539 genotypes studied in Zurn et al.
 170 (2022)²⁸ (shaded dots) with 3,215 SNP markers. Accessions are colored according to geographical/breeding
 171 origin. (I) Heterozygosity coefficients across different geographical/breeding origins when combining
 172 accessions from the diversity panel and 1,569 genotypes from Hardigan et al. (2021b)⁴.
 173 Genetic groups 1, 2 and 3 are colored in green, purple and orange, respectively. Groups 1, 2, 3: Heirloom &
 174 related, European mixed group and American & European mixed groups, respectively.

175

176 **Fruit quality traits in the diversity panel**

177 A total of 12 fruit quality traits were investigated in the panel of 223 accessions (Table 1). Traits were
 178 related to fruit weight (FW); fruit appearance (COL, skin color; UCOL, uniformity of skin color; UFS,
 179 uniformity of fruit shape; ACH, position and depth of achenes); firmness (FIRM); composition (TA, titratable
 180 acidity; TSS, total soluble solids (Brix units), and BA, the deduced ratio (Brix/TA)); and skin properties (GLOS,
 181 glossiness; SR, skin resistance; BRU, bruisedness). Analyses were carried out over two consecutive years,
 182 with the exception of the FIRM and SR traits, which were assessed over a single year (Table 1).

183 Most of the traits exhibited a considerable range of variation in the diversity panel, with coefficients of
 184 variation ranging from 3.7% for COL to 58.2% for skin resistance. For example, FW (average: 12.5 g) ranged
 185 from 1.8 and 32 g. (Table 1). Most traits showed a normal distribution, while SR, GLOS, UFS and BRU
 186 showed a skewed distribution (Fig. S6). Nine traits displayed high amount of genotypic variance associated
 187 with high broad sense heritability (H^2) ranging from 0.66 (ACH) to 0.98 (FIRM); H^2 of four traits, namely UFS
 188 (0.26), UCOL (0.43), BA (0.54) and BRU (0.57), was below 0.6 (Table 1). Few variations of H^2 between groups
 189 were observed for FW and FIRM, suggesting that phenotypic variability was equivalent between groups,
 190 whereas a strongest decrease in H^2 was observed for GLOS and BRU in G3 (Table 1). A significant interaction
 191 between genotype and environment was detected for all the traits for which repeated measurements were
 192 available over two years (Table 1), with the effect of environment being strongest for traits related to fruit
 193 composition (TSS, TA, BA).

194 To further explore the phenotypes of the diversity panel, we performed a PCA of the 223 accessions using a
 195 PCA biplot (Fig. 2A). PC scores revealed that the three genetic groups were distributed differently according
 196 to PC1 (39.2%) and PC2 (17.2%) in terms of fruit quality traits. G1 was distinct from G2 and G3 (Fig. 1B, Fig.
 197 S7A). Examination of the loadings of the traits on PC1 further showed that FW, appearance (UFS, UCOL),
 198 FIRM and skin properties (GLOS, SR and BRU) traits were responsible for the separation between G1 on one

199 side and G2 and G3 on the other side. TSS, TA and ACH had a very small contribution to the differentiation
 200 of the three subpopulations along PC1, and mostly contributed to PC2 and PC3, respectively (Fig. 2A, Fig.
 201 S7B).

202

203 **Table 1.** Summary statistics of the 12 fruit quality traits evaluated on the diversity panel in 2020 and 2021.
 204 n, number of accessions; CV, Coefficient of Variation; H², broad sense heritability; H²G1, H²G2, H²G3, broad
 205 sense heritability within each genetic group; %GE, percentage of genotype-by-environment interactions in
 206 the total variance; r² structure, structuration of the trait as the coefficient of determination of the linear
 207 regression between the trait values and the genetic groups. 20-21 indicates the combined values across
 208 two years, 2020 and 2021. ns, not significant genotypic effect.

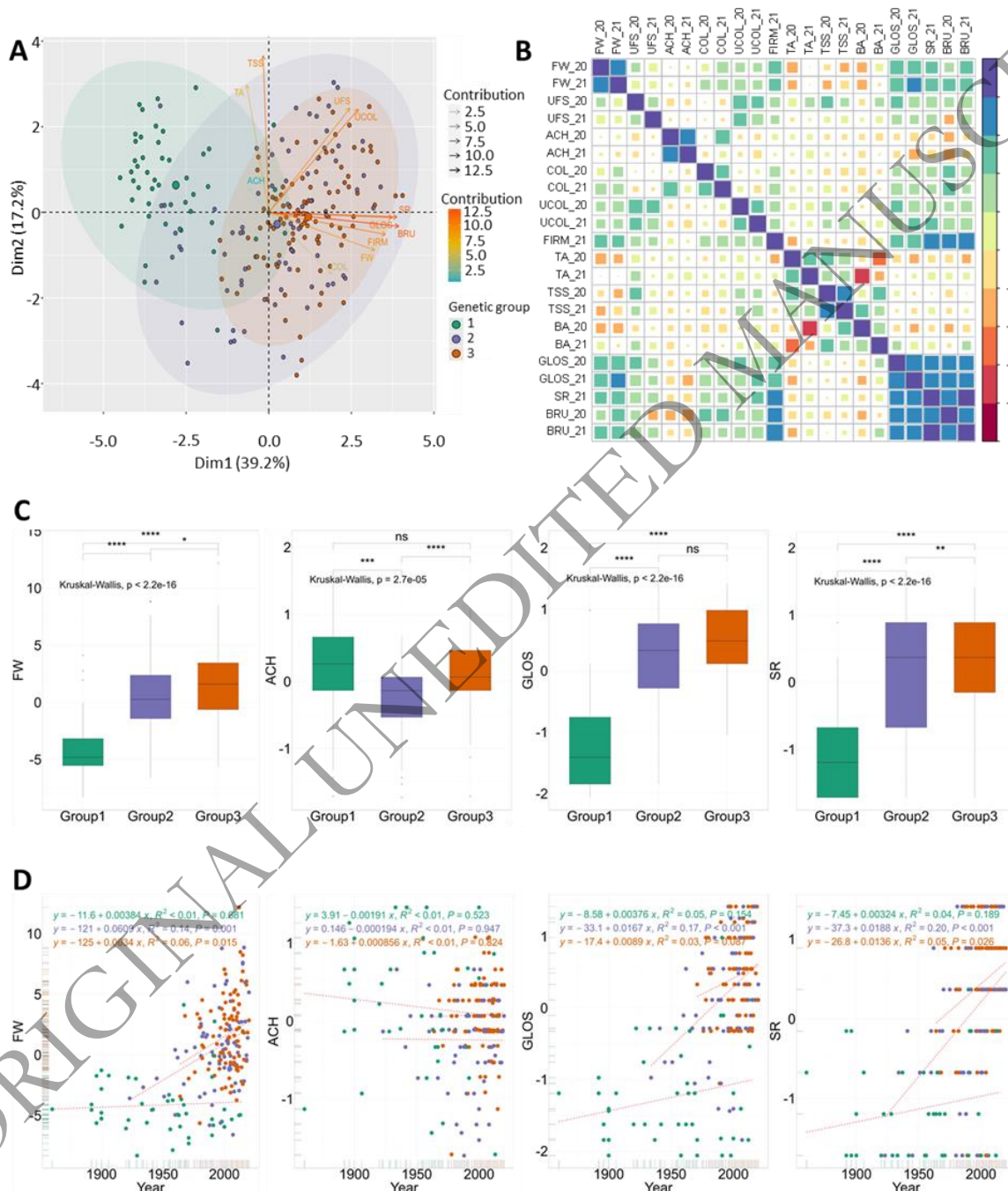
Trait	Year	n	Range	Mean	σ	CV	H ²	H ² G1	H ² G2	H ² G3	%GE	r ² structure
Fruit weight (FW, in g)	2020	169	1.8 - 30.9	12.4	5.4	43.6	0.96					
	2021	169	2.0 - 32.0	12.6	5.6	44.5	0.92					
	20-21	169	1.8 - 32.0	12.5	5.5	44.1	0.81	0.71	0.68	0.71	23.4	0.30
Shape uniformity (UFS)	2020	208	1 - 5	2.7	1.3	48.0	-					
	2021	197	1 - 5	3.1	1.3	41.5	-					
	20-21	208	1 - 5	2.9	1.3	44.9	0.26	ns	0.50	ns		0.05
Achene position (ACH)	2020	209	1 - 5	3.5	0.8	23.3	-					
	2021	198	1 - 5	3.2	0.9	28.8	-					
	20-21	209	1 - 5	3.4	0.9	26.2	0.66	0.71	0.67	0.60		0.08
Skin color (COL)	2020	201	1 - 7	1.2	4.507	3.7	-					
	2021	209	1 - 7.5	1.2	4.535	3.8	-					
	20-21	209	1 - 7.5	1.2	4.522	3.8	0.68	0.77	0.67	0.60		0.03
Color uniformity (UCOL)	2020	208	1 - 5	3.0	1.3	42.7	-					
	2021	198	1 - 5	2.8	1.3	47.0	-					
	20-21	208	1 - 5	2.9	1.3	44.9	0.43	ns	0.59	0.32		0.10
Firmness (FIRM, in kg/mm)	2020	-	-	-	-	-	-					
	2021	210	1.04 - 0.07	0.433	0.2	40.3	0.98	0.94	0.97	0.95		0.44
	20-21	-	-	-	-	-	-					
Titratable acidity (TA, in g/L)	2020	195	0.7 - 2.3	1.4	0.3	20.6	0.83					
	2021	175	0.4 - 2.0	1.2	0.3	24.1	0.91					
	20-21	195	0.4 - 2.3	1.3	0.3	23.1	0.70	ns	0.85	0.82	34.5	0.03
Total soluble solids (TSS, in Brix)	2020	207	3.6 - 11.0	7.1	1.4	19.7	0.92					
	2021	184	3.2 - 11.8	6.9	1.5	22.1	0.94					
	20-21	207	3.2 - 11.8	7.0	1.5	20.9	0.78	0.68	0.83	0.75	30.2	0.04
Brix/acidity ratio (BA)	2020	195	2.9 - 7.9	5.1	1.0	19.9	0.87					
	2021	175	2.1 - 12	5.6	1.5	27.5	0.95					
	20-21	195	2.1 - 12	5.3	1.3	24.8	0.54	ns	0.85	0.51	48.5	0.00
Glossiness (GLOS)	2020	195	1 - 5	3.5	1.2	35.8	-					
	2021	182	1 - 5	3.5	1.1	31.8	-					
	20-21	195	1 - 5	3.5	1.2	33.8	0.77	0.76	0.64	0.43		0.48
Skin resistance (SR)	2020	-	-	-	-	-	-					
	2021	210	0 - 3	1.65	1.0	58.2	-					0.34
	20-21	-	-	-	-	-	-					
Bruisiness (BRU)	2020	199	1 - 5	2.5	1.3	50.8	-					
	2021	54	0 - 5	1.8	1.0	54.3	-					
	20-21	199	0 - 5	1.9	1.1	55.7	0.57	0.52	0.45	ns		0.49

209

210

211 Correlation analysis of fruit quality trait data collected over 2020 and 2021 (Fig. 2B, Table S2) supported the
 212 relationships identified in the PCA biplot (Fig. 2A). GLOS, SR and BRU traits were positively and strongly
 213 correlated with each other and with FW and FIRM ($r=0.51$ to 0.87), indicating the strong potential for

214 directional selection of these traits (Fig. 2A). UFS and UCOL were also highly correlated among them
 215 ($r = 0.64$) and, to a lesser extent ($r = 0.35$ and 0.26), with FW. TSS and TA were significantly correlated
 216 ($r = 0.45$) but, within groups, the correlation was only significant for G2 ($r = 0.51$) and G3 ($r = 0.47$) groups
 217 (Fig. S8). FW also demonstrated significant negative correlations with TSS ($r = -0.21$) and TA ($r = -0.15$) (Fig.
 218 2B; Table S2). No or weak correlations were observed between ACH and other fruit quality traits.
 219



220
 221 **Figure 2.** Phenotypic variations across the three genetic groups of the panel. (A) Principal Component
 222 Analysis of the 2-year BLUP values for 11 traits. (B) Correlations between the 12 traits for each year. (C)
 223 Comparisons of 2-year BLUP values for FW, ACH, GLOS and SR among genetic groups. (D) Genetic gains for

224 FW, ACH, GLOS and SR among genetic groups. Genetic groups 1, 2 and 3 are colored in green, purple and
225 orange, respectively. Groups 1, 2, 3: Heirloom & related, European mixed group and American & European
226 mixed groups, respectively. FW, fruit weight; UFS, uniformity of fruit shape; COL, skin color; UCOL,
227 uniformity of skin color; ACH, position and depth of achenes; FIRM, firmness; TA, titratable acidity; TSS,
228 total soluble solids; GLOS, glossiness; SR, skin resistance; BRU, bruisedness.

229
230 Most fruit quality traits have undergone significant phenotypic changes over time, as old varieties have
231 evolved into modern cultivars (Figs 2C, 2D, Fig. S9). Phenotypic values of all fruit quality traits, except BA
232 and COL, were significantly different between the three genetic groups. For example, FW considerably
233 increased during the modern breeding phase, as reflected mainly in trends within G2 and G3 (Figs 2C, 2D).
234 G1 was associated with low FW, dull, soft, low SR and easily wounded skin with uneven color and shape,
235 whereas G3 exhibited the highest values for these traits (Fig. 2C, Fig. S9). G2 was equivalent to G3 for UFS
236 and UCOL, TSS and TA, and GLOS; and was in the average of G1 and G3 for FW, FIRM, SR and BRU. Cultivars
237 from G2 displayed more outcropped achenes than the others (Fig. 2C, Fig. S9).

238 These changes are linked to significant genetic gains over time for most fruit quality traits, with the
239 exception of ACH and BA (Fig. 2D, Fig. S10). For G2 and G3, the traits most affected along the breeding
240 cycles were fruit appearance (GLOS, Fig. 2D; UFS and UCOL, Fig. S10), fruit resilience to transport and
241 postharvest storage (SR, Fig. 2D; BRU and FIRM, Fig. S10) and fruit weight (FW, Fig. 2D). These traits are
242 important for consumers, retailers and growers respectively. A negative, non-significant trend was however
243 observed for TSS and TA, whose values were lower in G2 and G3 than in G1 (Fig. S9). Remarkably,
244 regardless of the TSS and TA reduction in modern varieties compared to old varieties, no significant
245 differences for BA values were observed between groups (Fig. S9).

246 While positive and time-dependent genetic gains were observed within G2 and G3, genetic gains were
247 usually low or inexistent within G1. For FW, for example, several recent varieties of the G1 showed the
248 same trait values as old ones. The absence of major improvements for such traits in modern cultivars
249 belonging to G1 is probably due to a low selection pressure, as the main selection objective was to produce
250 ornamental plants with pink flowers ('Frel' and 'Toscana') or white fruits ('Anablanca',
251 'Blanche_du_Morvan', 'F_Eure_et_Loire').

252

253 **GWAS of fruit quality traits**

254 To reveal the genetic architecture of fruit quality in strawberry, we performed GWAS on the 12 fruit quality
255 traits assessed in the 223 accessions of the strawberry diversity panel using genome-wide SNP markers
256 from the 50K FanaSNP array²². The structuration of the population (Figs 2B, 2C) was considered by fitting
257 both kinship and structure as cofactors for GWAS analysis. Detailed Manhattan plots for all 12 traits are

258 shown in Figs 3, 4, Fig. S11. The 71 significant associations with SNP markers are distributed on 51
259 chromosomal regions spread on 23 chromosomes (Table S3).

260

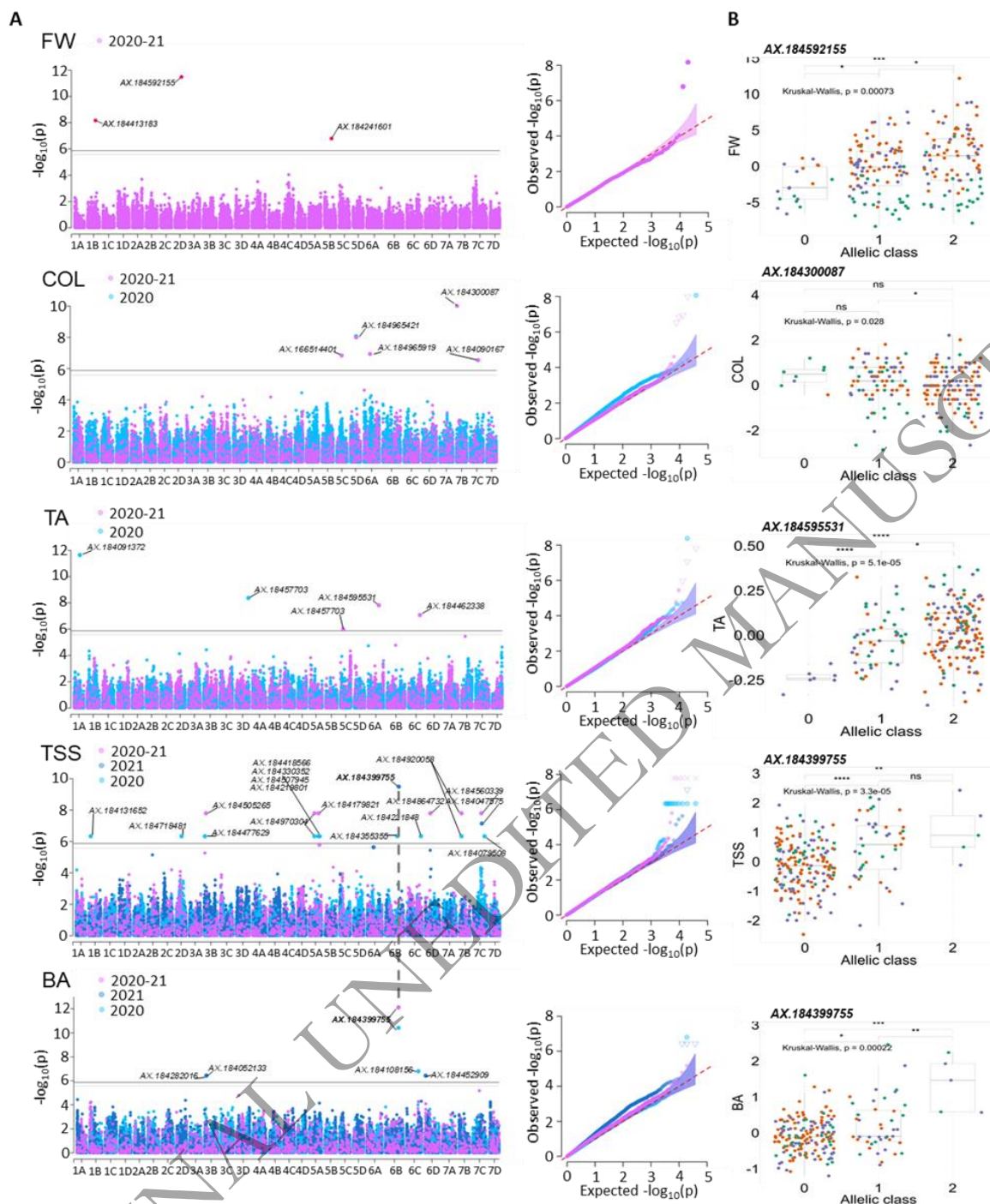
261 *Fruit weight and appearance (FW, UFS, COL, UCOL, ACH).*

262 Three significant SNP were identified for FW on chromosome 1B (19,119,571 bp, p-value 6.74E-09), 5B
263 (17,045,086 bp, p-value 1.60E-06) and a highly significant SNP on chromosome 2D (15,565,564 bp, p-value
264 3.27E-12) (Fig. 3A, Table S3). The minor allele of AX-184592155 had a phenotypic variance explained (PVE)
265 of 11.8% with an effect of 1.8g on FW (Fig. 3B, Table S3). Sixteen unique significant SNPs were identified for
266 appearance traits, eight for UFS, three for ACH and five for COL (Fig. 3A, Fig. S11, Table S3). No signal was
267 detected for UCOL.

268

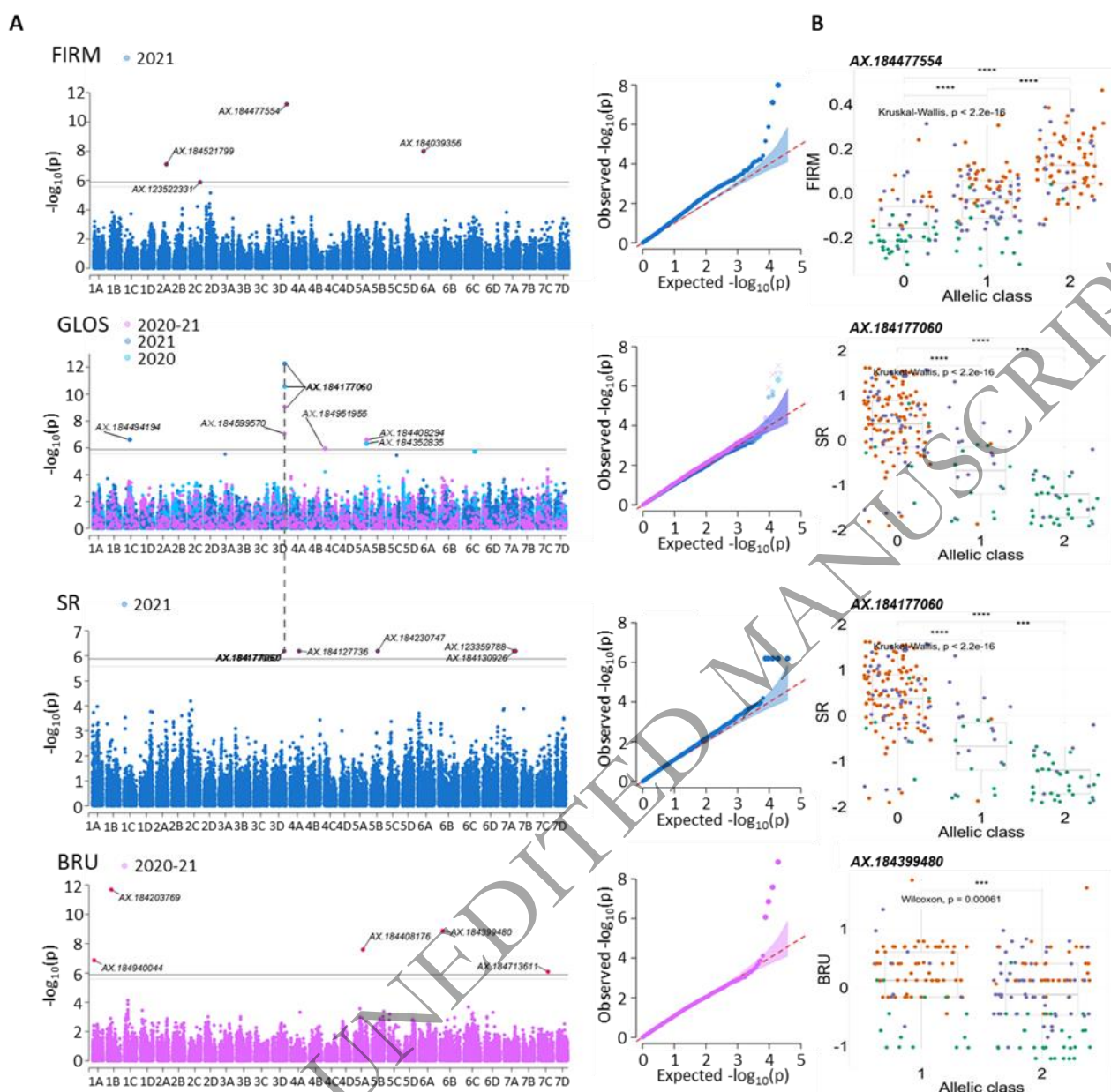
269

ORIGINAL UNEDITED MANUSCRIPT



270
 271
 272
 273
 274
 275
 276
 277

Figure 3. Genome wide association study of FW, COL, TA, TSS and BA. (A) Manhattan and Q-Q plots for yearly and 2-year BLUP values. (B) Effect of the most significant SNP marker. Genetic groups 1, 2 and 3 are colored in green, purple and orange, respectively. Groups 1, 2, 3: Heirloom & related, European mixed group and American & European mixed groups, respectively. FW, fruit weight; COL, skin color; TA, titratable acidity; TSS, total soluble solids; BA, brix acidity ratio. Marker classes are as follows: 0=AA genotype, 1=AB, and 2=BB genotype according to the Axiom™ Strawberry FanaSNP 50k.



278

279

280

281

282

283

284

285

286

287

288

289

290

Figure 4. Genome wide association study of FIRM, GLOS, SR and BRU. (A) Manhattan and Q-Q plots for yearly and 2-year BLUP values. (B) Effect of the most significant SNP marker. Genetic groups 1, 2 and 3 are colored in green, purple and orange, respectively. Groups 1, 2, 3: Heirloom & related, European mixed group and American & European mixed groups, respectively. FIRM, firmness; GLOS, glossiness; SR, skin resistance; BRU, bruisedness. Marker classes are as follows: 0=AA genotype, 1=AB, and 2=BB genotype according to the Axiom™ Strawberry FanaSNP 50k.

Fruit composition (TA, TSS, BA).

Twenty-seven unique significant SNPs were detected for fruit composition traits, five for TA, 18 for TSS and five for BA (Fig. 3A, Table S3). The SNP AX-184595531 detected for TA on the 2020-2021 combined values (25,621,066 bp, p-value 1.55E-08) was particularly notable for its PVE of 35.5%. Only seven cultivars, all belonging to G2, were unfavorable homozygous for this marker (Fig. 3B). SNPs AX-184091372 on

291 chromosome 1A (13,540,517 bp, p-value 2.30E-12, PVE 17.1%) and AX-184457703 on chromosome 3D
292 (25,621,066 bp, p-value 4.22E-09, PVE 17.9%) were also of particular interest for their PVE and impacting
293 effect on TA in 2021. AX-184399755 was the highest effect SNP for TSS in 2021 on chromosome 6B
294 (31,578,303 bp, p-value 3.24E-10, PVE 19%) (Fig. 3B). It was also highly significant for BA in 2020 (p-value
295 3.84E-11, PVE 46.1%) and 2020-2021 combined values (p-value 7.88E-13, PVE 65.8%) (Fig. 3B). Only five
296 cultivars were favorable homozygous for this marker. Interestingly, the SNP markers associated with the
297 TSS QTL on 6B (AX-184399755) and 6D (AX-184864732), and 7B (AX-184920058) and 7C (AX-184079508),
298 were found very close on the diploid *F. vesca* reference genome (*F. vesca* v4.0.a1³³), at 606,797 bp (Fvb6)
299 and 449,220 bp (Fvb7) from each other respectively.

300

301 *Fruit firmness and skin properties (FIRM, GLOS, SR, BRU).*

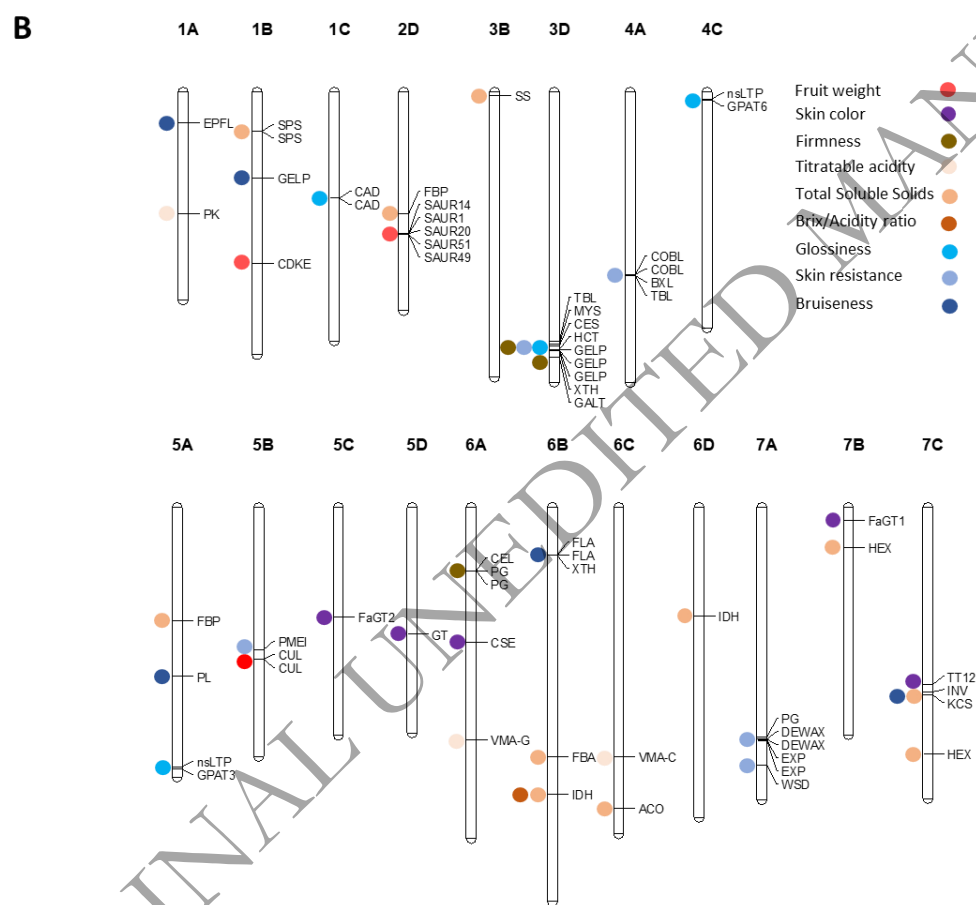
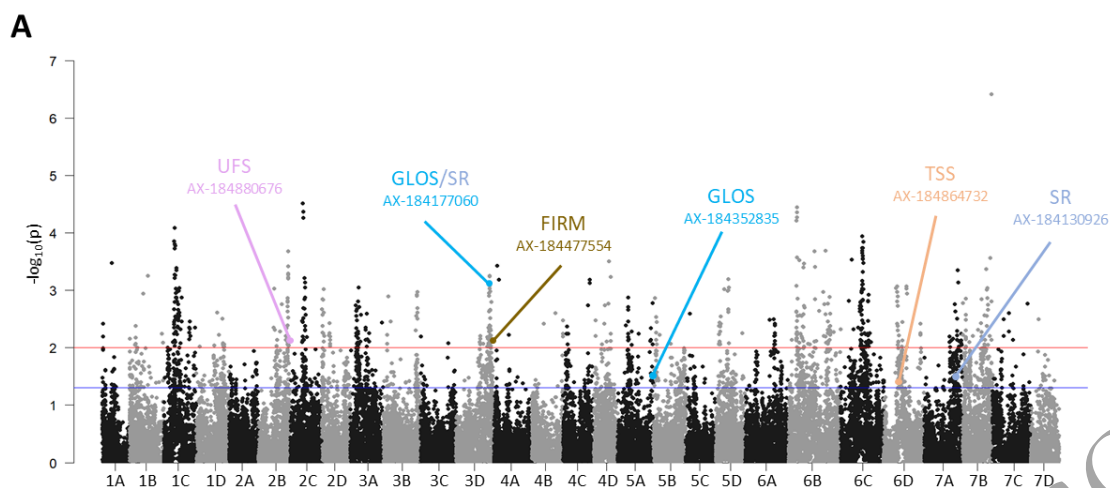
302 Four significant SNPs were detected for FIRM, six for GLOS, five for SR and five for BRU (Fig. 4A, Table S3).
303 The chromosome 3D was of particular interest for these traits as it comprises one highly significant SNP for
304 FIRM (29,275,014 bp, p-value 6.07E-12, PVE 11.2%) and the highly significant SNP AX-184177060
305 (27,845,440 bp) common to both GLOS (p-value 9.01E-10, PVE 26.2% on combined values) and SR (p-value
306 6.45E-07, PVE 8.4%) (Fig. 4B). The latter SNP was detected systematically in 2020, 2021 and 2020-2021 for
307 GLOS with PVE ranging from 26.2% to 28.7%, with a negative effect of the minor allele (-0.7 to -0.8 on 1 to 5
308 scale). MAF of this SNP was highly reduced towards G3, indicating strong selection of the favorable allele
309 (Fig. 4B). SNPs for BRU were detected for the 2020-2021 combined values only.

310

311 **Selective sweep signals during strawberry improvement**

312 We identified markers under selection during strawberry improvement in light of genome scans based on
313 Mahalanobis distance across the diversity panel (Fig. 5A) and nucleotide diversity throughout the genome
314 for all of the accessions in the diversity panel (Fig. 1F, Fig. S3). Six significant associations of SNP markers
315 with fruit quality QTL were detected, including one for UFS, one for FIRM, one for TSS, two for GLOS and
316 one for SR (Fig. 5A, Table S4). The AX-184177060 marker associated with GLOS and SR (chromosome 3D),
317 the AX-184477554 associated with FIRM (chromosome 3D), and the AX-184864732 (chromosome 6D)
318 associated with TSS, are found in chromosomal regions displaying a drastic reduction in nucleotide diversity
319 in modern genotypes (Fig. 1F, Fig. S3, Table S4). For example, in the case of the SNP marker AX-184177060
320 associated with the SR and GLOS QTL, the favorable allele is over-represented in the most recent accessions
321 (average year of release 2000), whereas cultivars heterozygous or unfavorably homozygous for the marker
322 were released around 1967 and 1947 respectively. This finding supports the fact that the favorable allele
323 has been selected over time.

324



325

326

327

328

329

330

331

332

Figure 5. Selective sweeps and candidate genes. (A) Selective sweeps as a Manhattan plot of p-values of the genome scan based on Mahalanobis distance. Red and blue lines indicate thresholds at 0.01 and 0.05, respectively. Only significant (p-value < 0.05) SNP markers associated with fruit quality QTL are represented. UFS, uniformity of fruit shape; GLO, glossiness; SR, skin resistance; FIRM, firmness; TSS, Total soluble solids. (B) Physical mapping of the candidate genes underlying the GWAS of nine traits on the Camarosa genome. Full names and abbreviations of candidate genes are given in Table 2.

333
334 **Candidate genes were identified for 37 QTL controlling 9 fruit quality traits**

335 Candidate genes (CG) underlying fruit quality QTL were identified within a window of ~400 kb surrounding
336 the QTL marker. This value, which corresponds to the short-range LD found in the California cultivars of *F. ×*
337 *ananassa*⁴, is stringent compared to the average LD calculated on the 28 linkage-groups in our diversity
338 panel, which is 932 kb. In chromosomal regions harboring strong QTL of interest and displaying low genetic
339 diversity and high LD, i.e. the 3D region extending from 23,233 to 29,635 kb (Fig. 1F), we considered much
340 larger intervals based on LD estimates (up to ~1,382 kb) for 3B and 3D. We excluded two traits (UFS and
341 ACH) from CG analysis because the molecular pathways underlying these traits are far from being
342 deciphered in strawberry. No QTL was detected for UCOL. In total, we identified 64 candidate loci for 37
343 SNP markers associated with the nine fruit quality traits (Fig. 5B). Table 2 provides names, abbreviations
344 and positions on Camarosa and Royal Royce genomes of these 64 CG. Their possible functions are indicated
345 in Table S5.

346
347 **Table 2.** Candidate genes underlying nine fruit quality traits. PVE, Phenotypic variance explained (%).
348 Position Camarosa and Position Royal Royce: physical positions on Camarosa and Royal Royce reference
349 genomes. Protein encoded by the candidate gene (CG): annotation in the Camarosa genome. CG Position
350 Camarosa and *F.x ananassa* identity: physical position and identity in the Camarosa genome. Published
351 GWAS/QTL: QTL detected with Affymetrix strawberry arrays on the same chromosomal regions as in this
352 study. *, CG found outside ~400 kb intervals around SNP markers.

353

355

356 **Discussion**

357

358 **Genetic and phenotypic shifts in modern strawberry breeding programs**

359 Our study sheds light on the genetic and phenotypic shifts that occurred over the last 160 years of
360 strawberry breeding by analyzing 223 accessions comprising original old and modern European breeding
361 material. According to our analyses, old strawberry cultivars, which here consist mainly of European
362 cultivars selected before 1950 and included in the Heirloom & related group (G1), are clearly separated
363 from other genetic resources (Fig. 1C), in agreement with earlier studies³² confirmed in recent papers^{4,34}.
364 For over half a century³⁵, breeding programs in Western and Southern Europe have made extensive use of
365 California cultivars and, more recently, of Florida cultivars, which are underrepresented in our study, as
366 progenitors. As a consequence, our results show the clustering of most European recent cultivars in an
367 American & European mixed group (G3). The European mixed group (G2), which includes other European
368 cultivars, is likely related to the group previously named Cosmopolitan⁴. European cultivars were also
369 separated from US cultivars in the Zurn et al. (2022) study²⁸ due to the large number of American
370 accessions.

371

372 The overall nucleotide diversity is well-conserved among the genetic groups of our panel (Fig. 1E). In
373 contrast, a significant erosion of genetic diversity was observed in highly structured populations^{4,5,29}. We
374 found a more nuanced picture by examining nucleotide diversity at the chromosome level, since it drops
375 dramatically in regions potentially subject to selection pressure (Fig. 1F, Fig. S3). The decrease in both LD
376 and heterozygosity specifically observed in the most recent American cultivars⁴ is likely explained by the
377 gradual differentiation of California and Florida populations. In contrast, cultivars and advanced lines of
378 Invenio as well as the recent European cultivars released after 1980 display higher heterozygosity values
379 (Fig. 1I). One possible explanation for the high genetic diversity retained in European accessions is that
380 European breeders had to cope with a wide range of breeding targets due to the diversity of cultural
381 practices, markets and consumer preferences found in Europe^{6,36}. High quality strawberry varieties released
382 in Europe therefore had to meet the requirements of both high cultivar performance, e.g. high fruit yield,
383 as in California cultivars⁵ and high sensory fruit quality, e.g. high flavor⁶.

384

385 Remarkably, recent studies have shown that despite a loss in genetic diversity, increases in both genetic
386 gain and phenotypic variation were observed in highly structured populations such as those of the
387 California breeding programs⁵. In these programs, breeding efforts rapidly led to the improvement of fruit
388 weight and fruit firmness^{5,27,29}, which participated to the so-called California green revolution⁵. European
389 breeding programs have benefited from these efforts, as modern American cultivars appear in the pedigree

390 of prominent European cultivars³. Consistently, our results indicate a similar trend towards improved fruit
391 size and firmness, as well as skin glossiness and resistance, in recent European germplasm (Fig. 2C, Fig. S9).
392 Interestingly, we found that TSS and TA values decreased over time in G1 but that the BA ratio kept the
393 same value (Figs S9, S10), in agreement with Feldmann et al. (2024)⁵ who even observed an increase in BA
394 levels, which could partly counterbalance the decrease in fruit sweetness. Antagonism between yield and
395 firmness, on one side, and TSS and TA, on the other side, was previously reported^{5,27,31}.

396

397 **Novel markers for the selection of fruit quality traits**

398 GWAS is a powerful tool for the detection of SNP markers linked to different traits in strawberry^{9,17,29,31,37,38}.
399 Here, based on a large diversity panel, we detected 71 marker-associations to major fruit quality breeding
400 targets. Some of the marker/QTL associations detected confirm published results and, consequently,
401 validate our findings in a different genetic context. In comparison with the GWAS/QTL published
402 data^{4,15,17,29,31,39,40,41} obtained using the Affymetrix strawberry arrays, only two common fruit quality QTL
403 located on the same chromosomal regions were detected here (Table 2). Our AX-184039356 marker linked
404 to FIRM on 6A is very close to those previously described for fruit firmness^{4,17,31,39}. Likewise, our AX-
405 184477629 marker linked to TSS on 3B is in the same chromosomal region as the SSC1 QTL controlling
406 soluble solids content³¹. In contrast, several previously reported QTL such as a FW QTL on 5B^{29,41}, a TSS QTL
407 on 5A⁴¹, a TA QTL on 5A¹⁵ have been found on the same chromosomes but in different regions. The genetic
408 diversity of unique European accessions included in our study allowed us to reveal new QTL and associated
409 SNP markers, even for well-studied fruit quality traits such as FW and TSS.

410

411 In contrast to these well-studied traits, few studies have unveiled the genetic architecture of skin
412 associated traits such as fruit glossiness^{17,42} which is, alongside color, one of the most prominent traits for
413 fruit attractiveness to the consumer⁴³. Remarkably, of the six associations found among the selective
414 sweeps detected, two were found for GLOS and one for SR (Fig. 5A). Furthermore, by highlighting a ~6,400
415 kb region on chromosome 3D linked to glossiness, skin resistance and firmness, our results shed a new light
416 on a genomic region under strong breeding pressure (Figs 1F, 5A). Remarkably, among the six associations
417 found among candidate selective sweeps, two were found for GLOS and one for SR. This chromosomal
418 region has thus probably played a crucial role in improving the attractiveness and post-harvest qualities of
419 strawberries, a feature that is receiving increasing attention in strawberry breeding programs. Information
420 on the position of SNP markers on both Camarosa and Royal Royce genomes will facilitate new studies on
421 fruit quality traits, thus contributing to validate these markers for MAS.

422

423 **Candidate genes**

424

425 *Fruit weight and appearance*

426 Fruit weight (FW) and shape are complex traits. Underlying genes of previously unknown functions have
427 been identified by map-based cloning in species such as tomato⁴⁴ and corresponding CG have been
428 detected in several crops⁴⁵. Translation of these findings to strawberry may however prove difficult because
429 of the different ontogenic origin of strawberry, which is an accessory fruit derived from the flower
430 receptacle and not from the ovary. Indeed, our GWAS study did not detect any known gene families linked
431 to fruit weight and shape, but highlighted for FW QTL several CG (*CDKE*, a cluster of five *SAUR*, *CUL*)
432 involved in cell division and expansion processes and their regulation (Table S5).

433
434 Red-colored anthocyanins, which give strawberries their attractive bright red appearance, are flavonoids
435 derived from the phenylpropanoid pathway. In cultivated strawberry, allelic variants of the master
436 regulator *MYB10* belonging to the MBW complex have been shown to be responsible for the white skin-
437 color and red flesh-color^{8,11}. In our GWAS study, we did not detect any previously known color QTL nor CG
438 linked to the MBW complex, probably because white fruit genotypes and flesh-color trait were under-
439 represented in our analysis. However, our diversity panel has enabled us to reveal new skin color QTLs and
440 identify strong CG involved in the successive steps leading to anthocyanin accumulation in strawberry¹¹: (i)
441 anthocyanin biosynthesis; (ii) formation of stabilized anthocyanidin-glucosides; and (iii) transport of
442 anthocyanidin-glucosides for storage in the vacuole. Color CG, which deserve further study, include a gene
443 (*CSE*) encoding shikimate esterase, an enzyme involved in lignin pathway that may compete with
444 anthocyanin biosynthesis for common substrates; several genes encoding glycosyltransferases (*GT*), among
445 which the strawberry FaGT1 enzyme that has been shown to generate anthocyanidin 3-O-glucosides⁴⁶ and
446 its homolog FaGT2; and a gene encoding a vacuolar flavonoid/H⁺-antiporter (*TT12*) that can actively
447 transport cyanidin-3-O-glucoside to the vacuole⁴⁷.

448
449 *Fruit firmness and composition*

450 Breakdown of the cell wall (CW) is the main mechanism responsible for fruit softening during ripening. CW
451 is mainly constituted by a cellulose-hemicellulose network immersed in a pectin matrix. Strawberry fruit
452 softening involves the pectin-degrading enzymes polygalacturonase (PG) and pectate lyase (PL)⁴⁸. The
453 down-regulation of *PL*⁴⁹ and of *PG*⁵⁰ influences fruit firmness and/or shelf life of strawberry. Many
454 additional proteins are involved in CW modifications e.g. pectin methylesterase (PME) and its inhibitors
455 (PMEI) that control cell adhesion and elasticity through pectin esterification, enzymes of the xyloglucan
456 endotransglycosylase/hydrolase (XTH) family involved in hemicellulose remodelling, cellulases (CEL) that
457 degrade cellulose, and expansins (EXP) that promote CW loosening. Other enzymes such as cellulose
458 synthase (CES) or proteins with ill-defined roles such as arabinogalactan-proteins (AGPs) likely play a role in
459 CW structure and properties. Therefore, considerable variations in fruit firmness can be expected by

460 modulating the activity of enzymes encoded by CG underlying the 3D QTL (*GALT*, *XTH*, *CES*) and 6A (*CEL*,
461 *PG*) QTL. *XTH* and *CES* are strong candidates located at 750 to 1,280 kb from the AX-184477554 marker in
462 the well-conserved 3D region while *CEL* and *PG* underly the 6D FIRM QTL previously detected⁴.

463

464 The sugar/acid balance is central for consumers perception of fruit quality¹⁹ and the sugar/acid ratio has
465 been widely adopted as a breeding target⁵. The major soluble sugars that accumulate during fruit ripening
466 are glucose, fructose and sucrose, the concentration of which depends on the cultivar⁵¹. The major organic
467 acids are malate and especially citrate, which is the predominant organic acid⁴⁸. Their concentrations are
468 stable or decrease during fruit ripening. Fruit sweetness is usually assessed in refractometer (Brix units),
469 which measures total soluble solids (TSS), including sugars and organic acids. Fruit acidity is assessed by TA,
470 to which citrate contributes most in strawberry. The accumulation in strawberry of soluble sugars and
471 organic acids depends on synthesis in the leaf (source) and long-distance transport of photoassimilates
472 (sucrose, inositol) to the fruit (sink). Photosynthetic sugars are further metabolized in the fruit to produce
473 soluble sugars and organic acids that are then stored in the vacuoles⁵². Our GWAS study identified several
474 CG implicated in the metabolism of sugars, either in the leaves or in the fruit, including *SPS* (1B QTL), *FBP*
475 (2D and 5A QTL), *SS* (3B QTL), *FBA* (6B QTL), and *INV* (7C QTL). The starch synthase (*SS*) is located more than
476 1 Mb apart from the 3B QTL marker but has been recently identified as a CG for a TSS QTL³¹. The neutral
477 invertase (*INV*), which underlies the major 7C TSS QTL (PVE 7.7%), is a strong candidate that has been
478 shown to be crucial for glucose and fructose accumulation during ripening in tomato⁵³ while a cell wall
479 invertase is responsible for a major TSS QTL in this species⁵⁴. Another strong candidate is the hexose
480 transporter (*HEX*) (7B and 7C QTL), which could transport glucose and fructose across the tonoplast, as
481 suggested in grape berries⁵⁵. Furthermore, the *HEX* gene may underlie two possible TSS homoeo-QTL
482 located on chromosomes 7B and 7C, respectively.

483

484 Two CG underlying TSS QTL encode enzymes involved in the tricarboxylic acid (TCA) cycle, notably isocitrate
485 dehydrogenase [NAD] (*IDH*) (6B QTL) and aconitase (*ACO*) (6C QTL). TCA is the central metabolic cycle that
486 uses substrates from the glycolysis to produce energy. It fulfills major roles in the fruit, among which the
487 metabolism of citric acid⁵⁶. While aconitase has been shown to contribute to the regulation of acidity in the
488 citrate-accumulating lemon⁵⁷, we did not detect any TA QTL corresponding to the 6C Brix QTL. Interestingly,
489 *IDH* underlies strong shared QTL for TSS (PVE=19.0) and BA (PVE=65.8) on chromosome 6B. The implication
490 of *IDH* a significant contributor to the TCA cycle, in the sugar/acid balance of strawberry, therefore merits
491 further studies. Moreover, *IDH* is also located at ~ 675 kb from the TSS QTL on chromosome 6D, indicating
492 that it could underlie two TSS homoeo-QTL located on chromosome 6B and 6D, respectively. As previously
493 suggested¹³, the detection of homoeo-QTL could depend on environmental conditions, which vary
494 according to the year of study.

495

496 The CG underlying the 1A TA QTL encodes pyruvate kinase (PK) a crucial enzyme for gluconeogenesis which
497 has already been demonstrated to regulate citric acid metabolism during strawberry fruit ripening⁵⁶. Two
498 additional CG for the TA QTL located on 6A (PVE 35.3%) and 6C (PVE 6.8%) encode subunits of the V-type
499 proton ATPase (*VMA-G* and *VMA-C*), respectively. Both are strong candidates for the control of fruit acidity,
500 as they are part of a protein complex whose role is to generate a proton gradient across the tonoplast,
501 which is essential to drive the storage of organic acids in the vacuole of fleshy fruits⁵⁸.

502

503

Skin properties

504

505 The outermost wall of the fruit is composed of the cuticle, the epidermis and several layers of sub-
506 epidermal cells⁵⁹. This ill-defined tissue, also called fruit skin⁶⁰, acts as a barrier against water-loss and
507 pathogens and provides protection against mechanical injuries⁶¹. Its properties depend on epidermal and
508 sub-epidermal cell patterning (cell size and shape) and on the composition and structure of CW and cuticle.
509 To date, the cuticle has been poorly studied in strawberry, except for its composition⁶². Recent studies, in
510 particular in the tomato model, furthered our understanding of the synthesis of cuticle components (wax
511 and cutin polyester, phenolics) and explored the complex interactions between cutin polyesters, CW
512 polysaccharides and phenolics, and their possible contribution to cuticle properties⁵⁹.

512

513 Fruit glossiness is an environment-sensitive trait linked to wax and cutin accumulation on the fruit surface
514 but also to epidermal cell patterning⁶³. Among CG identified for GLOS QTL are genes involved in
515 phenylpropanoid pathways (*CAD* in 1C QTL), epidermal patterning (*TBL* in 3D QTL), regulation of wax
516 biosynthesis (*MYS*, 3D QTL), lipid and cutin biosynthesis (*GPAT6*, 4C QTL; *GPAT3*, 5A QTL) and possibly
517 transport of cutin precursors (*InsLTP*, 4C and 5A)^{61,64}. In addition to the *MYS* gene, a transcription factor
518 involved through *DEWAX* in the regulation of the *ECERIFERUM1* (*CER1*) enzyme involved in the biosynthesis
519 of wax alkanes⁶⁵, this region harbors, within ~700 kb of 3D QTL markers, the phenolic pathway *HCT* gene
520 that is essential for cuticle formation⁶⁶ and, close-by, three *GELP* genes. Several members of the large *GELP*
521 family have been demonstrated to play crucial roles in cutin polymerization (cutin synthase⁶⁷) and in
522 assembly-disassembly of the related polyester suberin⁶⁸. Examination at the Tomato eFP Browser
523 (<http://bar.utoronto.ca>) and TEA-SGN (<https://tea.solgenomics.net>) databases of the expression of the
524 three closest tomato homologs (*Solyc03g005900*, *Solyc02g071610*, *Solyc02g071620*) of the 3D GLOS QTL-
525 linked *GELP* genes indicate that they are strongly expressed in the young fruit, when the cutin synthesis
526 rate is the highest⁶³. Furthermore, in the tomato pericarp, their expression is restricted to the outer and
527 inner epidermis. These findings strongly suggest that, in cultivated strawberry, a cluster of genes with likely
528 roles in cuticle formation and structure has been selected in modern varieties for its impact on fruit cuticle-
529 related traits, including GLOS.

530

531 Remarkably, we found that the major skin resistance (SR) QTL, which estimates the fragility of the fruit
532 surface to peel off when a mechanical stress is applied, is shared with the GLOS QTL on 3D. The major 3D
533 FIRM QTL (PVE 11.2%) was also found nearby (at ~1,400 kb). Since the FIRM trait was estimated by
534 measuring the force needed to punch a hole in the fruit surface (penetrometer), it can be linked to the
535 properties of the fruit skin. Interestingly, connections between fruit firmness and the cuticle have recently
536 been demonstrated in tomato where changes in cuticle composition and properties are responsible for a
537 major firmness QTL⁶⁹. Altogether, these results suggest that in the 3D conserved region, modifications of
538 fruit surface properties, either due to changes in epidermal cell patterning and/or in cell wall and cuticle
539 properties, have been selected in modern strawberry varieties for their effect on both fruit glossiness,
540 resistance to mechanical damages, and possibly firmness. Other candidates linked to either epidermis
541 patterning (*TBL* on 4A), cell wall modifications (*COBL* and *BXL* on 4A, *PMEI* on 5C, *PG* and *EXP* on 7A) and
542 cuticle formation (*DEWAX*, a target of *MYS*, and *WSD* on 7A) underly the additional SR QTL detected.

543

544 In contrast, none of the QTL detected for fruit bruisedness (BRU), a trait assessed visually, were found to
545 co-localize with either GLOS, SR or FIRM QTL while all these traits are strongly correlated, indicating that
546 the underlying mechanisms are probably different or that the corresponding QTL are below the detection
547 threshold. CW-related GC that may affect cell wall properties (*PL* on 5A, *XTH* on 6B) or cell adhesion of sub-
548 epidermal cells (*FLA* on 6B⁷⁰) merit further investigation, as fruit susceptibility to bruising is essential for
549 post-harvest handling and defense against fruit decay.

550

551 Conclusion

552 In summary, the exploration of untapped genetic resources, including European cultivars spanning 160
553 years of breeding, has revealed considerable changes in recent decades in the genetic and phenotypic
554 diversity of cultivated strawberry. American cultivars have had a major impact on recent European
555 breeding programs and, therefore, on modern strawberry varieties in Europe. However, our findings also
556 revealed that a considerable, and previously undescribed, genetic diversity can be harnessed for improving
557 fruit quality through breeding. Our study also highlights the contribution of fruit surface traits (glossiness,
558 skin resistance, bruisedness) to the development of modern varieties. The strong CGs underlying the main
559 QTL detected for these little studied traits warrant further investigations. This can be done, for example,
560 through additional association studies or functional analyses. From a more applied perspective, the genetic
561 markers highlighted will be used for the selection of improved strawberry varieties with high fruit quality.

562

563 Materials and methods

564

565 **Plant materials and experimental design**

566 A total of 223 accessions from the historical germplasm collection of Invenio was chosen to constitute the
 567 diversity panel. The trial took place in a soilless system, at Douville in the South-West of France (45° 1.2831'
 568 N; 0° 37.0198' E, France). The crop management was the one used for commercial semi-early cultivated
 569 strawberry in France. The trial was organized in a randomized complete block design of two blocks of four
 570 biological replicates each in a 288 m² glass greenhouse in 2020 and 2021. Planting of tray plants occurred
 571 around the 15th of December of the previous year.

572

573 **Sample preparation and phenotyping**

574 Fruits were harvested once per season and evaluated for 12 fruit quality traits: FW, fruit weight; UFS,
 575 uniformity of fruit shape; COL, skin color; UCOL, uniformity of skin color; ACH, position of achenes; FIRM,
 576 firmness; TA, titratable acidity; TSS, total soluble solids; BA, TSS/TA ratio; GLOS, glossiness; SR, skin
 577 resistance; BRU, bruisedness. FW was evaluated as the mean weight of harvested fruits after discarding
 578 immature and overripe fruits. UFS, UCOL, ACH as well as GLOS and BRU were visually assessed on 1-5 scales
 579 (Table 1) as a single note on a whole strawberry tray (>10 red ripe fruits). COL was evaluated on 4-5 red ripe
 580 fruits a 1-8 scale based on the strawberry color chart from Ctifl
 581 (<http://www.ctifl.fr/Pages/Kiosque/DetailsOuvrage.aspx?IdType=3&idouvrage=833>). FIRM was evaluated
 582 on six fruits from each accession with an FTA-GS15 (Güss) penetrometer (5 mm diameter) at 3 mm depth (5
 583 mm/s speed, 0.06kg release threshold). SR was evaluated on three fruits per accession on a 1-5 scale by
 584 applying an ascending pressure with the extremity of the thumb on the fruit surface. Bruisedness, which
 585 represents the susceptibility of the fruit to mechanical damages, was evaluated by visual inspection of the
 586 fruits 4 h after harvest. Analyses were performed for two consecutive years except for FIRM and SR traits
 587 which were evaluated a single year in 2021. TA and TSS were evaluated from a homogenized pool of a
 588 minimum of 10 fruits with a pH-metric titration with sodium hydroxide of 10 g fruit puree and an Atago
 589 Handheld (PAL-1) Digital Pocket Refractometer (Atago, Saitama, Japan), respectively.

590

591 **Statistical analysis**

592 Best Unbiased Linear Predictors (BLUPs) for the diversity panel were calculated using a linear mixed model
 593 (LMM) from the lme4 R package⁷¹:

594

$$y_{ijkl} = \mu + G_j + B_k + Y_l + (G : Y)_{il} + \epsilon_{ikl}$$

595

596 where Y/E represented the fixed effects of year/environments; B the fixed effect of blocks; G the
 597 random genotypic effect, with $G \sim N(0, \sigma^2_I)$; GxY/E the random genotype x year/environment effects, with
 598 $G \times Y/E \sim N(0, \sigma^2_{Y/E})$; ϵ the residual term, with $\epsilon \sim N(0, \sigma^2_e)$.

598

599 Variance components for these effects were estimated using restricted maximum likelihood (REML).

600 Broad sense heritability was estimated as follows:

$$H^2 = \frac{\sigma^2 G}{\sigma^2 G + \frac{\sigma^2 G:Y}{nyear} + \frac{\sigma^2 e}{nyear \times nrep.year}}$$

601 where genotype (G) variance at the numerator. Random variance components involving year (Y) were
602 divided by the mean number of years (*nyear*). Other random variance components involving block effects
603 or residuals were divided by the mean number of years times the mean number of replicates per year
604 (*nrep.year*).

605 Pearson correlation between different traits were calculated using 'cor' function and visualized by 'corrplot'
606 v. 0.92 R package. PCA on all traits was performed using the prcomp function from R core and visualized
607 with fviz_pca function from factoextra v.1.0.7 package or ggplot2 package. The impact of the structure on
608 each variable was assessed by simple regression of the genetic groups on their respective phenotypes.

609

610 Genotyping

611 DNA was extracted from young leaves with a CTAB method adapted from Sánchez- Sevilla *et al.*, (2015)³⁴.
612 Samples were genotyped using Affymetrix® 50K FanaSNP array²² in the 'Gentyane' genotyping platform
613 (Clermont-Auvergne-Rhône-Alpes, INRAE, France). SNP calling was processed through Axiom™ Analysis
614 Suite software (v5.1.1.1; Thermo Fisher Scientific, Inc.) following the best practices of the software
615 documentation. Accessions with missing data higher than 3% were removed from analysis. Markers
616 presenting more than 5% of missing data and minor allele frequencies of less than 5% were filtered out.

617

618 Structure and genetic diversity analysis

619 We performed a structure population analysis using STRUCTURE (v2.3.4⁷²) with 5 runs for a range of K = 2
620 to 10 with 38,120 markers. The burn-in period length was set to 10,000 and 20,000 Markov Chain Monte
621 Carlo (MCMC). The best fitting K was identified with STRUCTURE HARVESTER⁷³. Plots were performed using
622 the ggplot2 v.3.3.6 package⁷⁴. PCA analyses were performed with PCA function from factorMinerR v.2.7
623 package⁷⁵. Additionally, we included genotypes from Hardigan *et al.*, (2021b)⁴ and Zurn *et al.* (2022)²⁸ to
624 perform PCA using the prcomp function from R core and visualize with fviz_pca_ind function from
625 factoextra v.1.0.7 package or ggplot2 package. We conducted a ML tree with the 233 accessions using IQ-
626 TREE v.2.1.3⁷⁶ with 1000 bootstrap and the TVMe+ASC+R3 model suitable for SNP arrays. Linkage
627 disequilibrium for each chromosome and genetic group was computed using the LDcorSV v.1.3.3 package⁷⁷.
628 Nucleotide diversity among each genetic group was calculated using TASSEL⁷⁸. Finally, we performed
629 principal component analysis-based genomes scans to detect markers under selection using the pcadapt
630 package⁷⁹, implementing the pcadapt function with K = 3. Output from genome scans were then compared
631 with nucleotide diversity profiles to search for selective sweeps.

632

633 **Genome-Wide Association Study**

634 The association mapping was performed using GAPIT v.3⁸⁰ using the Camarosa genome physical positions¹
635 with the Bayesian-information and linkage-disequilibrium iteratively nested keyway (BLINK) model⁸¹. In
636 order to control for confounding effects, the structure was implemented for each trait in two different
637 ways by 1) adding the previously calculated structure parameters as covariates or 2) fitting directly principal
638 components from the principal component analysis using the PCA.total argument. Best models were
639 selected based on genomic inflation factors, λ . The kinship was determined from the SNP data using the
640 VanRaden mean algorithm. The analysis was performed on yearly and across two years Best Linear
641 Unbiased Predictors (BLUPs), using a 5% Bonferroni threshold. Manhattan and Quantile-Quantile plots
642 were plotted using the CMplot R package. Allelic effects for each significant marker were plotted on
643 adjusted means using the ggplot2 R package.

644

645 **Candidate gene mining**

646 Candidate genes (CG) underlying fruit quality QTL were identified in intervals of ~400 kb around the QTL
647 marker. This value, which corresponds to the short-range LD found in California cultivars of *F. × ananassa*⁴,
648 is stringent compared to the average LD of 932 kb calculated in our diversity panel. In chromosomal regions
649 harboring strong QTL of interest and displaying low genetic diversity and high LD, larger intervals (up to
650 1,382 kb) were considered. The annotations of genes located within the QTL interval were retrieved from
651 *F. × ananassa* cv. Camarosa reference genome assembly v1.0¹ and cv. Royal Royce haplotype-resolved
652 genome v1.0 assembly²³. Based on the authors' expertise in fruit biology, QTL intervals were first inspected
653 manually for genes belonging to categories possibly related to fruit quality traits, e.g. enzymes, transporters
654 and regulators of anthocyanin biosynthesis for fruit color^{11,14,18}, enzymes and regulators of wax and cutin
655 biosynthesis pathways for glossiness and skin resistance^{59,61,63,64,67}, and enzymes of primary metabolism,
656 organic acid transporters and proton pumps for titratable acidity^{13,51,82,83,84}. Their function in plant and fruit
657 was then investigated by exploiting the Arabidopsis database (<https://www.arabidopsis.org/>) with
658 corresponding TAIR accession numbers; the relevant literature, especially that relating to strawberry and
659 other fleshy fruit species of the *Rosaceae* family; and gene expression patterns in strawberry fruit using *F.*
660 *vesca* eFP browser⁸⁵. For skin-associated traits, patterns of gene expression in plant organs and fruit cell
661 types were further investigated in tomato, the fleshy fruit and cuticle model, using SGN-TEA
662 (<https://tea.solgenomics.net/>) and Tomato eFP browser
663 (http://bar.utoronto.ca/efp2/Tomato/Tomato_eFPBrowser2.html).

664

665 **Conflict of interest statement**

666 The authors declare that there are no conflicts of interest.

667

668 Author's contributions

669 BD and AIP conceived and designed the experiments. AIP conducted hands-on experiments and data
670 collection. AuP, JoP and JuP contributed to data collection. AIP, PRS, BD and CR analyzed the data. AIP, BD
671 and CR wrote the original draft. All authors read and approved the final manuscript.

672

673 Acknowledgements

674 We thank Sarah Touzani and Eva Bouillon for their help in phenotyping. The project was funded by the
675 Nouvelle-Aquitaine Region and the European Regional Development Fund (ERDF) (REGINA project no.
676 67822110; AgirClim project No. 2018-1R20202); and European Union Horizon 2020 research and innovation
677 program (BreedingValue project No. 101000747; PRIMA-Partnership 2019-2022 Med-Berry project). AIP
678 was supported by the CIFRE (Convention Industrielle de Formation par la Recherche) contract between
679 Invenio (SME, Bordeaux, France) and the INRAE BAP department.

680

681 Data availability

682 All relevant data generated or analyzed are included in the manuscript and the supporting materials.

683

684 References

685

- 686 1. Edger PP, Poorten TJ, VanBuren R, et al. Origin and evolution of the octoploid strawberry genome. *Nat*
687 *Genet.* 2019;51(3):541-547. doi:10.1038/s41588-019-0356-4
- 688 2. Whitaker VM, Knapp SJ, Hardigan MA, et al. A roadmap for research in octoploid strawberry. *Hortic*
689 *Res.* 2020;7:33. doi:10.1038/s41438-020-0252-1
- 690 3. Pincot DDA, Ledda M, Feldmann MJ, et al. Social network analysis of the genealogy of strawberry:
691 retracing the wild roots of heirloom and modern cultivars. *G3 (Bethesda)*. 2021;11(3):jkab015.
692 doi:10.1093/g3journal/jkab015
- 693 4. Hardigan MA, Lorant A, Pincot DDA, et al. Unraveling the Complex Hybrid Ancestry and Domestication
694 History of Cultivated Strawberry. *Mol Biol Evol.* 2021b;38(6):2285-2305. doi:10.1093/molbev/msab024
- 695 5. Feldmann MJ, Pincot DDA, Cole GS, Knapp SJ. Genetic gains underpinning a little-known strawberry
696 Green Revolution. *Nat Commun.* 2024;15(1):2468. Published 2024 Mar 19. doi:10.1038/s41467-024-
697 46421-6
- 698 6. Senger E, Osorio S, Olbricht K, et al. Towards smart and sustainable development of modern berry
699 cultivars in Europe. *Plant J.* 2022;111(5):1238-1251. doi:10.1111/tpj.15876
- 700 7. Liu Z, Liang T, Kang C. Molecular bases of strawberry fruit quality traits: advances, challenges, and
701 opportunities. *Plant Physiol.* 2023;kiad376. doi:10.1093/plphys/kiad376

- 702 8. Castillejo, C. et al. Allelic Variation of MYB10 is the Major Force Controlling Natural Variation of Skin
703 and Flesh Color in Strawberry (*Fragaria* spp.) fruit. *Plant Cell* 32, 3723-3749 (2020).
704 <https://doi.org/10.1105/tpc.20.00474>
- 705 9. Fan Z, Tieman DM, Knapp SJ, et al. A multi-omics framework reveals strawberry flavor genes and their
706 regulatory elements. *New Phytol.* 2022;236(3):1089-1107. doi:10.1111/nph.18416
- 707 10. Lara I, Belge B, Goulao LF. A focus on the biosynthesis and composition of cuticle in fruits. *J Agric Food*
708 *Chem.* 2015;63(16):4005-4019. doi:10.1021/acs.jafc.5b00013
- 709 11. Denoyes B, Prohaska A, Petit J, Rothan C. Deciphering the genetic architecture of fruit color in
710 strawberry. *J Exp Bot.* 2023;erad245. doi:10.1093/jxb/erad245
- 711 12. Zorrilla-Fontanesi Y, Cabeza A, Domínguez P, et al. Quantitative trait loci and underlying candidate
712 genes controlling agronomical and fruit quality traits in octoploid strawberry (*Fragaria* × *ananassa*).
713 *Theor Appl Genet.* 2011;123(5):755-778. doi:10.1007/s00122-011-1624-6
- 714 13. Lerceteau-Köhler E, Moing A, Guérin G, et al. Genetic dissection of fruit quality traits in the octoploid
715 cultivated strawberry highlights the role of homoeo-QTL in their control. *Theor Appl Genet.*
716 2012;124(6):1059-1077. doi:10.1007/s00122-011-1769-3
- 717 14. Labadie M, Vallin G, Petit A, et al. Metabolite Quantitative Trait Loci for Flavonoids Provide New
718 Insights into the Genetic Architecture of Strawberry (*Fragaria* × *ananassa*) Fruit Quality. *J Agric Food*
719 *Chem.* 2020;68(25):6927-6939. doi:10.1021/acs.jafc.0c01855
- 720 15. Rey-Serra P, Mnejja M, Monfort A. Shape, firmness and fruit quality QTLs shared in two non-related
721 strawberry populations. *Plant Sci.* 2021;311:111010. doi:10.1016/j.plantsci.2021.111010
- 722 16. Muñoz P, Castillejo C, Gómez JA, et al. QTL analysis for ascorbic acid content in strawberry fruit reveals
723 a complex genetic architecture and association with GDP-L-galactose phosphorylase. *Hortic Res.*
724 2023;10(3):uhad006. Published 2023 Jan 19. doi:10.1093/hr/uhad006
- 725 17. Cockerton HM, Karlström A, Johnson AW, et al. Genomic Informed Breeding Strategies for Strawberry
726 Yield and Fruit Quality Traits. *Front Plant Sci.* 2021;12:724847. Published 2021 Oct 5.
727 doi:10.3389/fpls.2021.724847
- 728 18. Labadie M, Vallin G, Potier A, et al. High Resolution Quantitative Trait Locus Mapping and Whole
729 Genome Sequencing Enable the Design of an Anthocyanidin Reductase-Specific Homoeo-Allelic Marker
730 for Fruit Colour Improvement in Octoploid Strawberry (*Fragaria* × *ananassa*). *Front Plant Sci.*
731 2022;13:869655. doi:10.3389/fpls.2022.869655
- 732 19. Gaston A, Osorio S, Denoyes B, Rothan C. Applying the Solanaceae Strategies to Strawberry Crop
733 Improvement. *Trends Plant Sci.* 2020;25(2):130-140. doi:10.1016/j.tplants.2019.10.003
- 734 20. Jin X, Du H, Zhu C, et al. Haplotype-resolved genomes of wild octoploid progenitors illuminate genomic
735 diversifications from wild relatives to cultivated strawberry. *Nat Plants.* 2023;10.1038/s41477-023-
736 01473-2. doi:10.1038/s41477-023-01473-2

- 737 21. Session AM, Rokhsar DS. Transposon signatures of allopolyploid genome evolution. *Nat Commun.*
738 2023;14(1):3180. Published 2023 Jun 1. doi:10.1038/s41467-023-38560-z
- 739 22. Hardigan MA, Feldmann MJ, Lorant A, et al. Genome Synteny Has Been Conserved Among the
740 Octoploid Progenitors of Cultivated Strawberry Over Millions of Years of Evolution. *Front Plant Sci.*
741 2020;10:1789. doi:10.3389/fpls.2019.01789
- 742 23. Hardigan MA, Feldmann MJ, Pincot DDA, et al. Blueprint for Phasing and Assembling the Genomes of
743 Heterozygous Polyploids: Application to the Octoploid Genome of Strawberry. *bioRxiv* 2021a; doi:
744 10.1101/2021.11.03.467115. [Preprint].
- 745 24. Lee HE, Manivannan A, Lee SY, et al. Chromosome Level Assembly of Homozygous Inbred Line
746 'Wongyo 3115' Facilitates the Construction of a High-Density Linkage Map and Identification of QTLs
747 Associated With Fruit Firmness in Octoploid Strawberry (*Fragaria × ananassa*). *Front Plant Sci.*
748 2021;12:696229. Published 2021 Jul 14. doi:10.3389/fpls.2021.696229
- 749 25. Han H, Barbey CR, Fan Z, Verma S, Whitaker VM, Lee S. Telomere-to-Telomere and Haplotype-Phased
750 Genome Assemblies of the Heterozygous Octoploid 'Florida Brilliance' Strawberry (*Fragaria ×*
751 *ananassa*). *bioRxiv* 2022.10.05.509768; doi: <https://doi.org/10.1101/2022.10.05.509768>.
- 752 26. Mao JX, Wang Y, Wang BT, Li JQ, Zhang C, Zhang WS, Li X, Li J, Zhang JX, Li H, Zhang ZH. High-quality
753 haplotype-resolved genome assembly of cultivated octoploid strawberry. *Horticulture Research.*
754 Volume 10, Issue 1, January 2023, uhad002, doi: 10.1093/hr/uhad002
- 755 27. Hummer K., Bassil NV., Zurn J., Amyotte B. Phenotypic characterization of a strawberry (*Fragaria*
756 *xananassa* Duchesne ex Rosier) diversity collection. *Plants, People, Planet.* 2022;5(2):209-224.
757 <https://doi.org/10.1002/ppp3.10316>
- 758 28. Zurn JD, Hummer KE, Bassil NV. Exploring the diversity and genetic structure of the U.S. National
759 Cultivated Strawberry Collection. *Hortic Res.* 2022;9:uhac125. Published 2022 May 26.
760 doi:10.1093/hr/uhac125
- 761 29. Fan Z, Whitaker VM. Genomic signatures of strawberry domestication and diversification. *Plant Cell.*
762 Published online December 19, 2023. doi:10.1093/plcell/koad314
- 763 30. Oh Y, Barbey CR, Chandra S, et al. Genomic Characterization of the Fruity Aroma Gene, FaFAD1,
764 Reveals a Gene Dosage Effect on γ -Decalactone Production in Strawberry (*Fragaria × ananassa*). *Front*
765 *Plant Sci.* 2021;12:639345. doi:10.3389/fpls.2021.639345
- 766 31. Fan Z, Verma S, Lee H, Jang YJ, Wang Y, Lee S, Whitaker VM. Strawberry soluble solids QTL with inverse
767 effects on yield. *Horticulture Research*, 2024; 11, uhad271, doi.org/10.1093/hr/uhad271
- 768 32. Horvath A, Sánchez-Sevilla JF, Punelli F, et al. Structured diversity in octoploid strawberry cultivars:
769 importance of the old European germplasm. *Annals of Applied Biology* 2011;159(3): 358-371
770 doi.org/10.1111/j.1744-7348.2011.00503.x

- 771 33. Edger PP, VanBuren R, Colle M, et al. Single-molecule sequencing and optical mapping yields an
772 improved genome of woodland strawberry (*Fragaria vesca*) with chromosome-scale contiguity.
773 *Gigascience*. 2018;7(2):1-7. doi:10.1093/gigascience/gix124
- 774 34. Sánchez-Sevilla JF, Horvath A, Botella MA, et al. Diversity Arrays Technology (DArT) Marker Platforms
775 for Diversity Analysis and Linkage Mapping in a Complex Crop, the Octoploid Cultivated Strawberry
776 (*Fragaria* × *ananassa*). *PLoS One*. 2015;10(12):e0144960. Published 2015 Dec 16.
777 doi:10.1371/journal.pone.0144960
- 778 35. Rosati P. Recent trends in strawberry production and research: an overview. *Acta Horticulturae*
779 1993;348, 23–44. DOI:10.17660/ActaHortic.1993.348.1
- 780 36. Mezzetti, B., Giampieri, F., Zhang, Y.T. & Zhong, C.F. Status of strawberry breeding programs and
781 cultivation systems in Europe and the rest of the world. *J. Berry Res.* 2018;8, 205-221.
782 DOI:10.3233/JBR-180314
- 783 37. Davik J, Aaby K, Buti M, et al. Major-effect candidate genes identified in cultivated strawberry
784 (*Fragaria* × *ananassa* Duch.) for ellagic acid deoxyhexoside and pelargonidin-3-O-malonylglucoside
785 biosynthesis, key polyphenolic compounds. *Hortic Res.* 2020;7:125. Published 2020 Aug 1.
786 doi:10.1038/s41438-020-00347-4
- 787 38. Nagamatsu S, Tsubone M, Wada T, et al. Strawberry fruit shape: quantification by image analysis and
788 QTL detection by genome-wide association analysis. *Breed Sci.* 2021;71(2):167-175.
789 doi:10.1270/jsbbs.19106
- 790 39. Muñoz P, Roldán-Guerra FJ, Verma S, Ruiz-Velázquez M, Torreblanca R, Oiza N, Castillejo C, Sánchez-
791 Sevilla JF, Amaya I. Genome-wide association studies in a diverse strawberry collection unveil loci
792 controlling agronomic and fruit quality traits. *bioRxiv* 2024;doi: 10.1101/2024.03.11.584394.
793 [Preprint].
- 794 40. Alarfaj R, El-Soda M, Antanaviciute L, et al. Mapping QTL underlying fruit quality traits in an F1
795 strawberry population. *The Journal of Horticultural Science and Biotechnology.* 2021;96(5), 634–645.
796 <https://doi.org/10.1080/14620316.2021.1912647>
- 797 41. Natarajan S, Hossain MR, Kim HT, et al. ddRAD-seq derived genome-wide SNPs, high density linkage
798 map and QTLs for fruit quality traits in strawberry (*Fragaria* × *ananassa*). *3 Biotech.* 2020;10(8):353.
799 doi:10.1007/s13205-020-02291-5
- 800 42. Sieczko L, Masny A., Pruski K., Żurawicz E., Mądry W. Multivariate assessment of cultivars' biodiversity
801 among the Polish strawberry core collection. *Hort. Sci. (Prague).* 2015;42: 83–93. doi:
802 10.17221/123/2014-HORTSCI
- 803 43. Lewers KS, Michael JN, Eunhee P, Yaguang L. Consumer preference and physiochemical analyses of
804 fresh strawberries from ten cultivars. *International Journal of Fruit Science.* 2020;20:sup2, 733-756,
805 DOI: 10.1080/15538362.2020.1768617

- 806 44. van der Knaap E, Chakrabarti M, Chu YH, et al. What lies beyond the eye: the molecular mechanisms
807 regulating tomato fruit weight and shape. *Front Plant Sci.* 2014;5:227. Published 2014 May 27.
808 doi:10.3389/fpls.2014.00227
- 809 45. Wu S, Zhang B, Keyhaninejad N, et al. A common genetic mechanism underlies morphological diversity
810 in fruits and other plant organs. *Nat Commun.* 2018;9(1):4734. Published 2018 Nov 9.
811 doi:10.1038/s41467-018-07216-8
- 812 46. Griesser M, Hoffmann T, Bellido ML, et al. Redirection of flavonoid biosynthesis through the down-
813 regulation of an anthocyanidin glucosyltransferase in ripening strawberry fruit. *Plant Physiol.*
814 2008;146(4):1528-1539. doi:10.1104/pp.107.114280
- 815 47. Marinova K, Pourcel L, Weder B, et al. The Arabidopsis MATE transporter TT12 acts as a vacuolar
816 flavonoid/H⁺ -antiporter active in proanthocyanidin-accumulating cells of the seed coat. *Plant Cell.*
817 2007;19(6):2023-2038. doi:10.1105/tpc.106.046029
- 818 48. Moya-León MA, Mattus-Araya E, Herrera R. Molecular Events Occurring During Softening of
819 Strawberry Fruit. *Front Plant Sci.* 2019;10:615. Published 2019 May 15. doi:10.3389/fpls.2019.00615
- 820 49. Jiménez-Bermúdez S, Redondo-Nevado J, Muñoz-Blanco J, et al. Manipulation of strawberry fruit
821 softening by antisense expression of a pectate lyase gene. *Plant Physiol.* 2002;128(2):751-759.
822 doi:10.1104/pp.010671
- 823 50. García-Gago JA, Posé S, Muñoz-Blanco J, Quesada MA, Mercado JA. The polygalacturonase FaPG1 gene
824 plays a key role in strawberry fruit softening. *Plant Signal Behav.* 2009;4(8):766-768.
825 doi:10.1104/pp.109.138297
- 826 51. Moing, A., Renaud, C., Gaudillère, M., Raymond, P., Roudeillac, P., & Denoyes-Rothan, B. Biochemical
827 Changes during Fruit Development of Four Strawberry Cultivars. *Journal of the American Society for*
828 *Horticultural Science* jashs 2001;126(4), 394-403. <https://doi.org/10.21273/JASHS.126.4.394>
- 829 52. Ruan YL. Sucrose metabolism: gateway to diverse carbon use and sugar signaling. *Annu Rev Plant Biol.*
830 2014;65:33-67. doi:10.1146/annurev-arplant-050213-040251
- 831 53. Miron D, Petreikov M, Carmi N, et al. Sucrose uptake, invertase localization and gene expression in
832 developing fruit of *Lycopersicon esculentum* and the sucrose-accumulating *Lycopersicon hirsutum*.
833 *Physiol Plant.* 2002;115(1):35-47. doi:10.1034/j.1399-3054.2002.1150104.x
- 834 54. Fridman E, Carrari F, Liu YS, Fernie AR, Zamir D. Zooming in on a quantitative trait for tomato yield
835 using interspecific introgressions. *Science.* 2004;305(5691):1786-1789. doi:10.1126/science.1101666
- 836 55. Afoufa-Bastien D, Medici A, Jeauffre J, et al. The *Vitis vinifera* sugar transporter gene family:
837 phylogenetic overview and macroarray expression profiling. *BMC Plant Biol.* 2010;10:245. Published
838 2010 Nov 12. doi:10.1186/1471-2229-10-245.

- 839 56. Yang M, Hou G, Peng Y, et al. FaGAPC2/FaPKc2.2 and FaPEPCK reveal differential citric acid metabolism
840 regulation in late development of strawberry fruit. *Front Plant Sci.* 2023;14:1138865. Published 2023
841 Apr 4. doi:10.3389/fpls.2023.1138865
- 842 57. Shlizerman L, Marsh K, Blumwald E, Sadka A. Iron-shortage-induced increase in citric acid content and
843 reduction of cytosolic aconitase activity in Citrus fruit vesicles and calli. *Physiol Plant.* 2007;131(1):72-
844 79. doi:10.1111/j.1399-3054.2007.00935.x
- 845 58. Huang XY, Wang CK, Zhao YW, Sun CH, Hu DG. Mechanisms and regulation of organic acid
846 accumulation in plant vacuoles. *Hortic Res.* 2021;8(1):227. Published 2021 Oct 25.
847 doi:10.1038/s41438-021-00702-z
- 848 59. Reynoud N, Petit J, Bres C, et al. The Complex Architecture of Plant Cuticles and Its Relation to Multiple
849 Biological Functions. *Front Plant Sci.* 2021;12:782773. Published 2021 Dec 10.
850 doi:10.3389/fpls.2021.782773
- 851 60. Bargel H, Neinhuis C. Tomato (*Lycopersicon esculentum* Mill.) fruit growth and ripening as related to
852 the biomechanical properties of fruit skin and isolated cuticle. *J Exp Bot.* 2005;56(413):1049-1060.
853 doi:10.1093/jxb/eri098
- 854 61. Petit J, Bres C, Mauxion JP, Bakan B, Rothan C. Breeding for cuticle-associated traits in crop species:
855 traits, targets, and strategies. *J Exp Bot.* 2017;68(19):5369-5387. doi:10.1093/jxb/erx341!
- 856 62. Järvinen R, Kaimainen M, Kallio H. Cutin composition of selected northern berries and seeds, *Food*
857 *Chemistry.* 2010;Volume 122, Issue 1, pages 137-144.
858 <https://doi.org/10.1016/j.foodchem.2010.02.030>
- 859 63. Petit J, Bres C, Just D, et al. Analyses of tomato fruit brightness mutants uncover both cutin-deficient
860 and cutin-abundant mutants and a new hypomorphic allele of GDSL lipase. *Plant Physiol.*
861 2014;164(2):888-906. doi:10.1104/pp.113.232645
- 862 64. Petit J, Bres C, Mauxion JP, et al. The Glycerol-3-Phosphate Acyltransferase GPAT6 from Tomato Plays a
863 Central Role in Fruit Cutin Biosynthesis. *Plant Physiol.* 2016;171(2):894-913. doi:10.1104/pp.16.00409
- 864 65. Liu Q, Huang H, Chen Y, et al. Two Arabidopsis MYB-SHAQKYF transcription repressors regulate leaf
865 wax biosynthesis via transcriptional suppression on DEWAX. *New Phytol.* 2022;236(6):2115-2130.
866 doi:10.1111/nph.18498
- 867 66. Kriegshäuser L, Knosp S, Grienberger E, et al. Function of the HYDROXYCINNAMOYL-CoA:SHIKIMATE
868 HYDROXYCINNAMOYL TRANSFERASE is evolutionarily conserved in embryophytes. *Plant Cell.*
869 2021;33(5):1472-1491. doi:10.1093/plcell/koab044
- 870 67. Girard AL, Mounet F, Lemaire-Chamley M, et al. Tomato GDSL1 is required for cutin deposition in the
871 fruit cuticle. *Plant Cell.* 2012;24(7):3119-3134. doi:10.1105/tpc.112.101055

- 872 68. Ursache R, De Jesus Vieira Teixeira C, Déneraud Tendon V, et al. GDSL-domain proteins have key roles
873 in suberin polymerization and degradation. *Nat Plants*. 2021;7(3):353-364. doi:10.1038/s41477-021-
874 00862-9
- 875 69. Li R, Sun S, Wang H, et al. FIS1 encodes a GA2-oxidase that regulates fruit firmness in tomato. *Nat*
876 *Commun*. 2020;11(1):5844. Published 2020 Nov 17. doi:10.1038/s41467-020-19705-w
- 877 70. Ma Y, Shafee T, Mudiyansele AM, et al. Distinct functions of FASCILIN-LIKE ARABINO GALACTAN
878 PROTEINS relate to domain structure [published correction appears in *Plant Physiol*. 2023 Aug
879 3;192(4):3203]. *Plant Physiol*. 2023;192(1):119-132. doi:10.1093/plphys/kiad097
- 880 71. Bates D, Mächler M, Bolker B, Walker S. Fitting Linear Mixed-Effects Models Using lme4. *Journal of*
881 *Statistical Software*. 2015;67:1–48. DOI:10.18637/jss.v067.i01
- 882 72. Pritchard JK, Stephens M, Donnelly P. Inference of Population Structure Using Multilocus Genotype
883 Data, *Genetics*. 2000;155: 945–959. <https://doi.org/10.1093/genetics/155.2.945>.
- 884 73. Earl, Dent A. and vonHoldt, Bridgett M. STRUCTURE HARVESTER: a website and program for visualizing
885 STRUCTURE output and implementing the Evanno method. *Conservation Genetics Resources*
886 2011;DOI: 10.1007/s12686-011-9548-7
- 887 74. Wickham H ggplot2: Elegant Graphics for Data Analysis. Springer-Verlag New York. 2016;ISBN 978-3-
888 319-24277-4. <https://ggplot2.tidyverse.org>.
- 889 75. Lê S, Josse J, Husson F. FactoMineR: A Package for Multivariate Analysis. *Journal of Statistical Software*.
890 2008;25(1), 1–18. doi:10.18637/jss.v025.i01
- 891 76. Minh BQ, Schmidt HA, Chernomor O, et al. IQ-TREE 2: New Models and Efficient Methods for
892 Phylogenetic Inference in the Genomic Era [published correction appears in *Mol Biol Evol*. 2020 Aug
893 1;37(8):2461]. *Mol Biol Evol*. 2020;37(5):1530-1534. doi:10.1093/molbev/msaa015
- 894 77. Mangin B, Siberchicot A, Nicolas S, Doligez A, This P, Cierco-Ayrolles C. Novel measures of linkage
895 disequilibrium that correct the bias due to population structure and relatedness. *Heredity (Edinb)*.
896 2012;108(3):285-291. doi:10.1038/hdy.2011.73
- 897 78. Bradbury PJ, Zhang Z, Kroon DE, Casstevens TM, Ramdoss Y, Buckler ES. TASSEL: software for
898 association mapping of complex traits in diverse samples. *Bioinformatics*. 2007;23(19):2633-2635.
899 doi:10.1093/bioinformatics/btm308
- 900 79. Luu K, Bazin E, Blum MG. pcadapt: an R package to perform genome scans for selection based on
901 principal component analysis. *Mol Ecol Resour*. 2017;17(1):67-77. doi:10.1111/1755-0998.12592
- 902 80. Wang J, Zhang Z. GAPIT Version 3: Boosting Power and Accuracy for Genomic Association and
903 Prediction. *Genomics Proteomics Bioinformatics*. 2021 Aug;19(4):629-640. doi:
904 10.1016/j.gpb.2021.08.005. Epub 2021 Sep 4. PMID: 34492338; PMCID: PMC9121400.

- 905 81. Huang M, Liu X, Zhou Y, Summers RM, Zhang Z. BLINK: a package for the next level of genome-wide
906 association studies with both individuals and markers in the millions. *Gigascience*. 2019 Feb
907 1;8(2):giy154. doi: 10.1093/gigascience/giy154. PMID: 30535326; PMCID: PMC6365300.
- 908 82. Causse M, Duffe P, Gomez MC, et al. A genetic map of candidate genes and QTLs involved in tomato
909 fruit size and composition. *J Exp Bot*. 2004;55(403):1671-1685. doi:10.1093/jxb/erh207
- 910 83. Etienne C, Rothan C, Moing A, et al. Candidate genes and QTLs for sugar and organic acid content in
911 peach [*Prunus persica* (L.) Batsch]. *Theor Appl Genet*. 2002;105(1):145-159. doi:10.1007/s00122-001-
912 0841-9
- 913 84. Etienne C, Moing A, Dirlewanger E, Raymond P, Monet R, Rothan C. Isolation and characterization of
914 six peach cDNAs encoding key proteins in organic acid metabolism and solute accumulation:
915 involvement in regulating peach fruit acidity. *Physiol Plant*. 2002;114(2):259-270. doi:10.1034/j.1399-
916 3054.2002.1140212.x
- 917 85. Hawkins C, Caruana J, Li J, et al. An eFP browser for visualizing strawberry fruit and flower
918 transcriptomes. *Hortic Res*. 2017;4:17029. Published 2017 Jun 21. doi:10.1038/hortres.2017.29
- 919
920
921